Cellulose nanocrystals isolated from South African invasive wood species

by

Kyle Raatz

Thesis presented in fulfilment of the requirements for the degree of Master of Science in Forestry and Wood Science the Faculty of AgriScience at Stellenbosch University

Supervisor: Prof. Martina Meincken
Co-supervisor: Dr. Marietjie Lutz

March 2018

Declaration

By submitting this thesis electronically, I declare that the entirety of the work contained therein is my own, original work, that I am the sole author thereof (save to the extent explicitly otherwise stated), that reproduction and publication thereof by Stellenbosch University will not infringe any third party rights and that I have not previously in its entirety or in part submitted it for obtaining any qualification.

December 2017

Abstract

The increased use of cellulose nanocrystals (CNC) due to their high strength, environmentally friendly and renewable source presents a possibility to add value to the potential waste product of South African invasive trees. This material, with its superior characteristics, has been used in a variety of applications including heart valves, microelectronics pumps and liquid crystal displays (LCD).

In this study CNCs obtained from two invasive hardwood species, namely acacia, eucalyptus were compared to CNCs isolated from commercial cellulose, with an unknown wood source and from pine, a softwood. CNCs were synthesised via acid hydrolysis and then characterised with Fourier Transformed Infrared Spectroscopy (FTIR), X-Ray Diffraction (XRD), Transmission Electron Microscopy (TEM), Dynamic light scattering (DLS), Atomic Force Microscopy (AFM) and Differential Scanning Calorimetry (DSC).

No clear difference was determined between hardwoods and softwoods and CNCs synthesised from invasive tree species were found to be similar, if not superior, to CNCs from commercial cellulose

Opsomming

Die toenemende gebruik van sellulose-nanokristalle (CNC) as gevolg van hul hoë sterkte, omgewingsvriendelike en hernubare bron, bied die moontlikheid om waarde toe te voeg tot die potensiële afvalproduk van Suid-Afrikaanse indringerbome. Hierdie materiaal, met sy voortreflike eienskappe, is gebruik in 'n verskeidenheid toepassings, insluitend hartkleppe, mikroelektroniese pompe en vloeibare kristal verskynings (LCD).

In hierdie studie is CNC's verkry uit twee indringer hardehoutsoorte, naamlik acacia, eucalyptus vergelyk met CNCs wat van kommersiële sellulose geïsoleer is, met 'n onbekende houtbron en van Denne, 'n sagtehout. CNC's is gesintetiseer deur suur hidrolise en dan gekenmerk deur Fourier Transformeerde Infrarooi Spektroskopie (FTIR), X-Straal Diffraksie (XRD), Transmissie-elektronmikroskopie (TEM), Dinamiese ligverspreiding (DLS), Atomiese Krag Mikroskopie (AFM) en Differensiële Skandeering Kalorimetrie (DSC).

Geen duidelike verskil is ondervind tussen hardehoutsoorte en sagtehout nie, en CNC's wat gesintetiseer is uit indringerboomspesies, is gevind dat dit soortgelyk is, indien nie beter nie, as CNCs uit kommersiële sellulose.

Acknowledgements

Although my name is on this thesis, I could not have succeeded if it was not for the support from my **colleagues, educators and friends**.

First and foremost, I give thanks to **God** for blessing me with opportunity and the ability to further my education, and for providing me with the strength to overcome mountains along my journey.

I would like to thank my supervisor **Prof. Martina Meincken** from Forestry and Wood Science, for her patience, encouragement, critique and support over the last two years. Thank you for gracing me with financial support, guidance and leadership.

To my co-supervisor **Dr. Marietjie Lutz** from Polymer Science, thank you for your help and support along this journey.

To my lab partners **Marehette Le Grange, Nelisa Dyayiya** and the rest of the **Oliefins lab group,** thank you for your knowledge, assistance and friendship.

To my **colleagues** at Forestry and Wood Science, thank you for all the fun, laughter and encouragement throughout our years together.

To my **family,** especially my mother**,** for their relentless support, positivity, joy and love as I journeyed down the road to achieve my Masters in Science.

To my **girlfriend,** thank you for being my rock-solid support, providing me with encouragement and love for these two years. You played a vital role in my academic career.

Lastly but not least, I would like to thank everyone for their essential contribution to this thesis:

The Department of Forestry and Wood Science

The Department of Polymer Science

Dr. Remy Butcher from iThemba Labs (WAXD)

Dr. A. Laurie from the Geology CAF facility (TEM)

Uncle Solly from the Department of Chemical Engineering

Divann Robertson and Neil Basson (DSC and FTIR)

Pauline Skillington from Mondi (DLS)

Lia Bester from the Department of Chemical Engineering (DLS)

Table of Contents

List of figures

List of tables

List of Equations

List of abbreviations

AFM	Atomic force microscopy
CNC	Cellulose nanocrystals
DLS	Dynamic light scattering
DP	Degree of polymerisation
DSC	Differential Scanning Calorimetry
FTIR	Fourier transform infrared spectroscopy
I_{α}	Alpha cellulose
I_{β}	Beta cellulose
I_{004}	Crystallite indices parallel to fibre axis
I_{110}	Crystallite indices perpendicular to fibre axis
$I_{11\bar{0}}$	Crystallite indices perpendicular to fibre axis
I_{200}	Crystallite indices perpendicular to fibre axis
$I_{amorphous}$	Amorphous index
IAP	Invasive alien plants
IWS	Invasive wood species
TEM	Transmission electron microscopy
T_M	Melting temperature
T_O	Onset degradation temperature
wt%	Weight percentage
XRD	X-ray diffraction

Chapter 1

Introduction and objectives

1.1. Introduction

Over the past few years cellulose nanocrystals (CNC), also known as cellulose nanowhiskers, have gained significant attention within the scientific community, due to the wide range of advantages these nano-structures have. CNCs are named after their high aspect ratio, rod-like structure. Research has shown that these highly crystalline synthetic nanoparticles vary in dimension with a length between 100 nm to several μm and a diameter of 5-50 nm, depending on the source (Durán *et al*., 2011; Kargarzadeh *et al*., 2012; Sofla *et al*., 2016). Cellulose sources can vary from plant based organisms; wood (Morelli *et al*., 2012), cotton (Morais *et al*., 2013), and bamboo (Chen *et al*., 2011) to some aquatic animals such as tunicate (Sofla *et al*., 2016).

One of the many advantages of cellulose is that it is abundantly available, a renewable resource, has a low production cost, is environmentally friendly due to its biodegradability, shows low toxicity, is transparent (Zhou *et al*., 2011) and has a Young's modulus comparable to some metals (aluminium and steel) and composite materials, like Kevlar (Orts *et al*., 2005) currently used in industry. The potential applications for CNCs are broad due to their many benefits. At present CNCs are predominantly being utilised as reinforcing polymer fillers due to their high elastic modulus and as reinforcing filler replacements for natural rubber (Zhang *et al*. 2014) and stimuli-responsive and mechanically adaptive composites (Hsu *et al*. 2011). Their low toxicity allows CNCs to be consumed and thus the medical industry incorporates CNCs in drug capsules, or as drug blinders (Villanova *et al*., 2011), they are used for artificial heart valves (Cherian *et al*., 2011) and as scaffolding for bone tissue (Zhou *et al*. 2013). Furthermore, in the electrical industry CNCs are incorporated into electrical devices to create, for example, super lightweight capacitors (Yang *et al*., 2015)

Wood is one of the main natural resources of cellulose. Wood is typically comprised of 18 – 35% lignin, 40 – 50% cellulose, 25 – 35% hemicelluloses and about 4 – 10% of organic extractives and inorganic minerals (Pettersen 1984). All plant based organisms consist of cells, which walls are made up of long cellulose chains. These chains form crystalline microfibrils, surrounded by amorphous regions. Both regions are linked together through strong hydrogen bonds. When these bonds are broken through an hydrolysis method, the amorphous region can be separated from the crystalline nanoparticles (Grange, 2015).

Cellulose can be isolated through various extraction processes such as chemical (Morelli et al., 2012), mechanical (Fall *et al*. 2014), enzymatic (Sacui *et al*., 2014), or a combination of these techniques and the properties of CNCs will vary with the isolation technique. The techniques can be applied optimally to separate the inter and intra fibril bonds to improve nanocellulose yield (Sacui *et al*., 2014) and change the surface properties and characteristics of CNCs (De Mesquita *et al*. 2010). Acid hydrolysis thus far is one of the most widely applied methods to obtain CNCs in an aqueous suspension.

South Africa is severely plagued with invasive plant species. The most concerning issue about these invasive plant species is that they transform the ecosystem by either consuming resources (nutrients, water and light) excessively, or by changing its environment to suit their own needs (i.e. change the pH value of the soil), which negatively impacts the natural environment (Richardson & Wilgen, 2004). The invasive tree species that affect South Africa the most are those that have no or very little natural deterrents. Among them are pine, acacia, eucalyptus, *arundo* and *salix* species (Nel *et al*., 2004). Pine and eucalyptus are used due to their commercial value, but most invasive species carry very little value and by law have to be cleared off the land. Producing CNCs from these species would add immense value to a resource that is ultimately regarded as waste.

This study investigates the properties, characteristics and feasibility of CNCs isolated from selected invasive South African tree species and compared them to commercially used CNCs.

1.2. Objectives

The main objective of this study was to investigate the properties and characteristics and feasibility of CNCs isolated from three South African invasive tree species, namely *Pinus radiata*, *Eucalyptus gomphocephala and Acacia cyclops* and compare them to CNCs produced from commercial cellulose.

If the properties of these CNCs prove to be comparable it would add immense value to the wood obtained from invasive trees that are essentially a waste material and by law have to be cleared.

As a secondary objective the Seifert alpha cellulose extraction method was adjusted to isolate alpha cellulose for the production of CNCs.

The main project steps were as follows:

1. Isolation of α-cellulose from invasive wood species.
2. Characterisation of α-cellulose.

3. Synthesis of CNCs from above α-cellulose and commercial α-cellulose.
4. Characterisation of CNCs.
5. Evaluation of properties and characteristics of the synthesised CNCs.
6. Comparison of the CNCs obtained from different sources

1.3 Thesis outline

The overview and structure of this thesis is as follows:

Chapter 1: Presents an introduction and overview of this study.

Chapter 2: Provides a brief history and literature review on the background of materials, analytical techniques and experimental procedures.

Chapter 3: Describes the experimental work and analytical procedures utilized in this study.

Chapter 4: Results and discussion

Chapter 5: Conclusion and future recommendations

Chapter 2

Literature Review

2.1. Colonisation and expansion of invasive wood species

The slow invasion of trees across the world is a natural process involving seed migration. In nature, tree seeds and fruits are transported via the wind, rivers, oceans and animals to various locations where they invade local and sometimes foreign soil over time (Pearson & Dawson, 2005; Pitelka, 1997). However, the invasion of alien species across the world has become faster and more effective in changing the environment, predominantly due to globalisation (Richardson & Wilgen, 2004). Throughout early stages of colonisation, trees were brought in from foreign countries for various applications, ranging from structural wood for building to farming purposes, such wind breaks and feed stocks (Pooley, 2009; Showers, 2010)

In recent times, government and private entities have created policies to combat the spread and reduce the impact of invasive alien plants (IAP) on the natural environments (DEA, 2014).The South Africa government in its fight against invasive species, has established the Department of Environmental Affairs (DEA) to govern the management of IAPs under the National Environmental Management: Biodiversity (NEM:BA) Act10 of 2004. It classifies invasive species into four main groups: Category 1a, 1b, 2 and 3, based on their commercial value and their ability to neutralise and become established within the South African ecosystem. Category 1a is declared the most invasive species, requiring immediate eradication. The working for water (WfW) programme was established in 1995 with the main goal to reduce the impact of IAPs on natural water resources in strategic catchment areas across all important biomes (DEA, 2014; Richardson & Wilgen, 2004)

The main reason why IAPs are difficult to control is that they spread and reproduce at a faster rate than they can be controlled (van Wilgen *et al*., 2012). They tend to out-compete their indigenous competitors, as they typically consume natural resources, such as nutrients, water and light at a faster rate (Richardson & Wilgen, 2004; Shaughnessy, 1980). It is also important to note that IAPs have the amazing ability of adapting to many environments and thus one invasive species could potentially affect many different native species (van Wilgen *et al*., 2004). If IAPs are not eradicated or controlled they could inhibit the development of less competitive native species, which may potentially lead to the extreme case where the native ecosystem is completely compromised (van Wilgen et al., 2004)

2.1.1 History to the introduction and discovery of invasive wood species in South Africa

The first recorded introduction of invasive wood species (IWS) to South African shores can be dated back to the first Dutch settlers in the 1600's. Jan van Riebeek imported seedling of alder *(Alnus glutinosa*), Norway spruce *(Picea abies),* Scots pine *(Pinus sylvestris),*ash (*Franxinus excelsior*) and oak *(Quercus robur)* to develop the Cape into a re-supply station for merchant ships and to grow construction wood to supply Europe and Asia (Pooley, 2009). Indigenous forest and woodland tree species are usually slow growing and would not have grown fast enough to supply the increasing demand. The earliest recording of a forest plantation was in 1694 by Simon van der Stel, who planted ash, oak and alder trees in the Cape gardens. At the end of the 1700's the majority of indigenous wood species around the Cape had been depleted. It was only in the 1800's that additional invasive species, meant for food stocks, such as vine and stone fruit trees, spread into South Africa to feed missionaries (Showers, 2010). The introduction of IWS into South Africa, from other continents, continued until the early 1900's as they are fast growing and more resilient than native trees. Even today they are used for construction material (pine, eucalyptus), tanning chemicals (*Acacia mearnsii* bark), farming purposes, such as wind restrictors (*Acacia dealbata, Eucalyptus gomphocephala, Casuarina cunninghamiana*) and vegetation cover (*Acacia saligna, Acacia cyclops*), or aesthetic appeal (*Jacaranda mimosifolia*) (DAFF, 2015; Henderson, 2007; van Wilgen et al., 2001). To date approximately 750 tree species were introduced into South Africa and around 110 of these IWS are deemed to be extremely invasive (van Wilgen et al., 2001). A case study shows that alien invasive species are spread across approximately 10.1 million ha of South Africa amounting to about 8.28% of the land (Le Maitre *et al*., 2000).

The most aggressive invasive wood species (IWS) across all South African biomes are *Acacia mearnsii* (Black wattle), *Acacia cyclops* (Rooikrans), *Acacia saligna* (Port Jackson), *Melia azedarach* (Syringa), Mesquite (*Prosopis spp.*) and the majority of the *Pinus, Hakea* and *Opuntia* species (Marais et al., 2001). For this study, wood from eucalyptus, acacia and pine was chosen.

2.2. Wood structure

Since the beginning of civilisation, humanity used wood as a fuel source and various other products including: construction material (poles, beams and boats), furniture, tools (handles, boards) and weapons (spears, warplanes in World War 2, etc.). Modern developments allow wood to be chemically and physically processed, broadening the number of possible applications to paper, veneer, particleboard, laminated timber, cellulose, microcrystalline cellulose and nano-cellulose.

Wood has several advantages: it is structurally strong relative to its weight, in contrast to other materials (cement, plastic, metals), it is thermally and electrically insulating, with low thermal deformation (contraction and expansion) (Samuel & Samuel 2010), provides signs of fatigue instead of immediate failure (Clorius, 2002; Tampone, 2007) and it is resistant to oxidation and low concentrations of acids. Wood is one of the fastest replenishing renewable resources in comparison to other natural sources (oil, coal and metal deposits, which are slowly being depleted), it is abundant in cellulose, environmentally friendly as it is biodegradable and lastly it is abundant around the earth (Martinez et al., 2005; Pérez et al., 2002; Tsoumis, 1991). However, wood also has disadvantages, which includes the following: it is hygroscopic and absorbs or desorbs moisture, thereby changing its dimensions, it degrades under natural conditions, it is anisotropic (most properties vary in different structural directions) and it has variable properties depending on ecological and genetics factors (Tsoumis, 1991).

Figure 2.1 shows the general features of wood: the rings containing earlywood and latewood, as well as the sapwood heartwood and the pith. The tissue is largely made up of hollow, porous, long cylindrical cells, known as tracheids or fibres (Clemons, 2010). These fibres are comprised mainly of cellulose and hemicelluloses filaments embedded in a matrix of lignin resisting compression (Maiti & Rodriguez, 2015). In addition to transporting water from the roots to the crown, the fundamental task of the wood cells is to provide the tree with enough strength to stand upright and to resist environmental stresses of the wind (Pittermann et al., 2006).

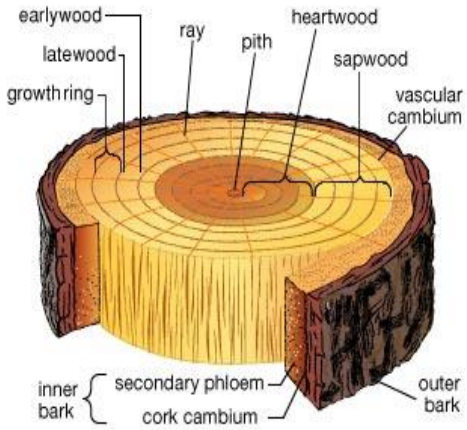

Figure 2.1: Wood cross-section reference (Museochies 2017)

Earlywood is formed during the main growth season and thus is influenced by external factors, such as water and nutrient availability (Cown & McConchie, 1981). The transition to latewood is induced during times of lower photosynthesis activity, when the cells in the cambial layers are less inclined to reproduce, or when the water availability decreases significantly. The latewood cells show a reduction in cell diameter and an increase in cell wall thickness. Therefore earlywood cells have a larger diameter and thinner walled cells than latewood, which has a narrow diameter thick walled cells (see figure 2.2) (Kudo et al., 2014; Tsoumis, 1991; Uggla et al., 2001)

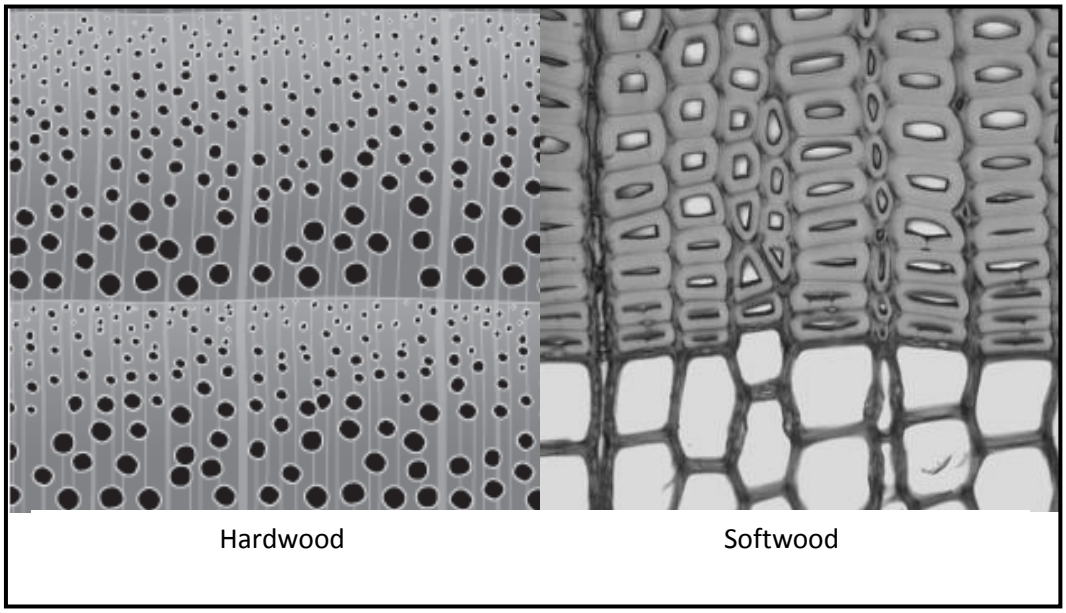

Figure 2.2: Transverse view of earlywood and latewood bands in softwoods (showing tracheids) and hardwoods (showing vessels) (Neagu *et al*. 2006; Nunlist 2012).

2.3. Wood classification

Trees are classified as softwood or hardwood, depending on their anatomical structure (Craig *et al*., 2005; Mazzarello, 1999). Softwood (Gymnosperms species or coniferous trees) are evergreen and have needle like leaves. To name a few, they include: pines, spruce, fir and yaw. Hardwoods (Angiosperms, or deciduous trees) have broad leaves and include acacia, eucalyptus and balsa ash (Craig *et al*., 2005), as displayed in Figure 2.3.

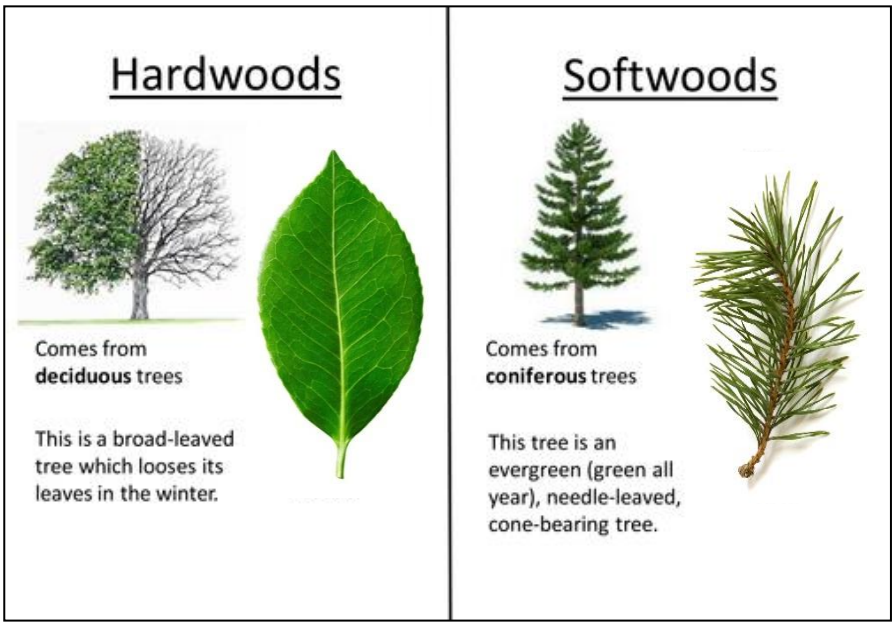

Figure 2.3: Botanical comparison between softwood and hardwood (Khatkar 2015)

Softwoods and hardwoods species display various cellular characteristics as shown in Figure 2.4.

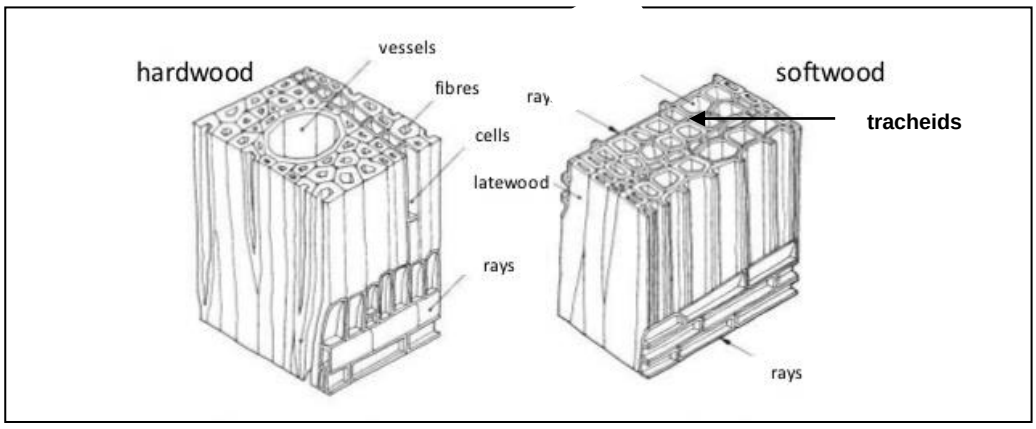

Figure 2.4: Cellular and structural differences between softwoods and hardwoods (Zakaria *et al*. 2013)

Softwoods consist of long and narrow tracheids, ray cells and parenchyma cells. Axial tracheids make up the majority (90%) of softwood cells and their length ranges from 3-8 mm with a diameter between 15 and 80 μm. Ray cells are oriented radially and are much smaller with a length of 100 to 200 μm and a low aspect ratio between 5-10:1 (Beck-Candanedo *et al*. 2005; Miller 1999; Tsoumis 1991). Parenchyma cells are the smallest of the cells found in softwoods, with a length between 100 and 220 μm and a diameter ranging from approximately 10 to 50 μm (Tsoumis, 1991).

A study conducted by Cown & McConchie (1981) showed that *Pinus radiata* tracheids vary on average between 3.3 to 4 mm in length.

Hardwoods consist of a greater variety of cells, comprising fibres, vessel elements, as well as ray and parenchyma cells. The hardwood fibres are long and narrow with pointed closed ends and are shorter than tracheids. Fibre dimensions depend on the species and range from 500 – 2500 μm in length and 10 – 50 μm in diameter (Shmulsky & Jones, 2011; Tsoumis, 1991). Research conducted by Lundqvist *et al*. (2017) showed that South African grown *Eucalyptus gomphocephala* fibres with a length between 600-800 μm and a diameter around 1mm on average.

Vessels are large water conducting elements that display a significant variation in dimensions, depending on external growth factors. Vessels short with an average length of 200-1300 μm and wide with a diameter ranging from 0.5 – 500 μm (Tsoumis, 1991), depending on the water availability of the growth site.

2.4. Cell wall structure

Wood cell walls are three layered structures made from cellulose, hemicelluloses and lignin, as illustrated in Figure 2.5. S_1 is the thin outer layer, S_2 is the middle layer and S_3 is known as the lumen wall (Kretschmann, 2003; Tsoumis, 1991).

Cell walls consist largely of crystalline cellulose chains, or microfibrils, surrounded by numerous amorphous regions. The microfibrils are randomly organised in the primary wall, nearly axially oriented in the S_2 layer and nearly horizontal in the S_1 and S_3 layers (John & Thomas 2008; Kretschmann 2003). The lumen is the hollow centre of the cell transporting fluids in the tree. All the cells are held together by an amorphous hemicelluloses and lignin layer known as the middle lamella (Martinez *et al*., 2005; Plomion *et al*., 2001).

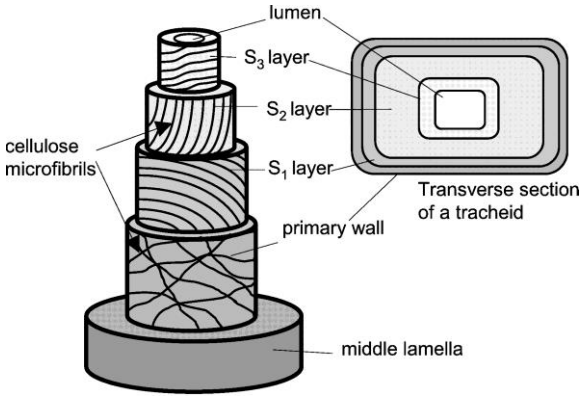

Figure 2.5: Three-dimensional structure of cell walls in wood (Plomion et al., 2001)

2.5 Chemical composition

The general chemical composition of wood is similar across all species. The fundamental elements that make up the majority of the wood are carbon (50%), hydrogen (6%), oxygen (44%) and trace amounts of other elements. These primary constituents merge to form larger organic compounds. The two main components are carbohydrates (cellulose, hemicelluloses) and phenolic substances, such as lignin, which constitute 65-75 and 18-35% of wood, respectively. Other components are extractives (proteins, starch, oils and waxes) and inorganic materials (ash), however they are only present in small amounts (Pettersen 1984; Thornber & Notrhcote 1961). Table 2.1 displays the general wood composition for softwoods and hard woods.

Component	Softwoods (%)	Hardwoods (%)
Cellulose	40-45	43-47
Hemicellulose	20-29	25-35
Lignin	25-35	17-25
Extractives	1-5	1-8

Table 2.1: General wood composition of hardwoods and softwoods (Khalil *et al.* 2012; Kumar *et al.* 2008; Tsoumis 1991)

2.5.1. Cellulose

Cellulose is predominantly a fibrous structure, which is made up of carbon, hydrogen and oxygen in the molecular form of $(C_6H_{10}O_5)_n$ (Oyeniyi & Itiola, 2012). Cellulose is a carbohydrate that is found primarily in the S_2 layer of wood cell walls and its amount varies between 40 – 50% from softwoods to hardwoods (Pettersen 1984). Thus it is one of the most abundantly produced organic

materials in the world, being grown at an estimated rate of 1.5 x 10^{12} tons annually (Kumar *et al. 2008*.

Cellulose is a monosaccharide consisting of insoluble linear chains of 1,4 linked β-D-glucopyranose units (John & Thomas, 2008; Pérez *et al*., 2002).The length of the repeated units is expressed as the number of glucose molecular constituents per cellulose chain, most commonly referred to as the degree of polymerisation (DP) (Hubbell & Ragauskas 2010; Pettersen 1984). The purest cellulose material, such as cotton, with a cellulose content of 90%,has a DP of up to 15000 units (Oyeniyi & Itiola 2012; Sabinesh *et al*. 2014) and wood with a cellulose content between 40 – 50% has an average DP between 8000-10 000 (Mckendry 2002; Pettersen 1984).

As illustrated in Figure 2.6, the glucose units comprise of three hydroxyl and hydrogen groups positioned perpendicular and parallel to its ring respectively. The pyranose ring is orientated into a chair conformation to accommodate the hydroxyl groups (Credou & Berthelot, 2015). The hydroxyl groups in particular play an important role in the mechanical properties of cellulose as it has the ability to form strong hydrogen bonds (John & Thomas, 2008).

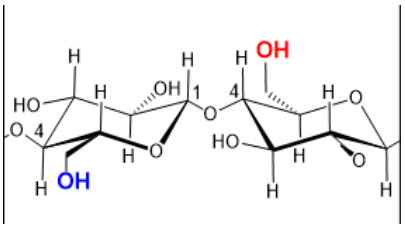

Figure 2.6**:** Illustration of a cellulose chain (Kaushik & Moores, 2016)

As wood cells grow, about 40 cellulose molecules self-assemble into larger chains known as elementary fibrils with a diameter of approximately 3.5 nm (Carrasco *et al*. 2011). The elementary fibrils then combine through Van der Waals forces (amorphous regions) and hydrogen bonds (crystalline regions) to larger, cylindrical structures, called microfibrils, with a diameter of 10-30 nm (see Figure 2.7) (John & Thomas 2008; Lynd *et al*. 2002; Wang *et al*. 2007).

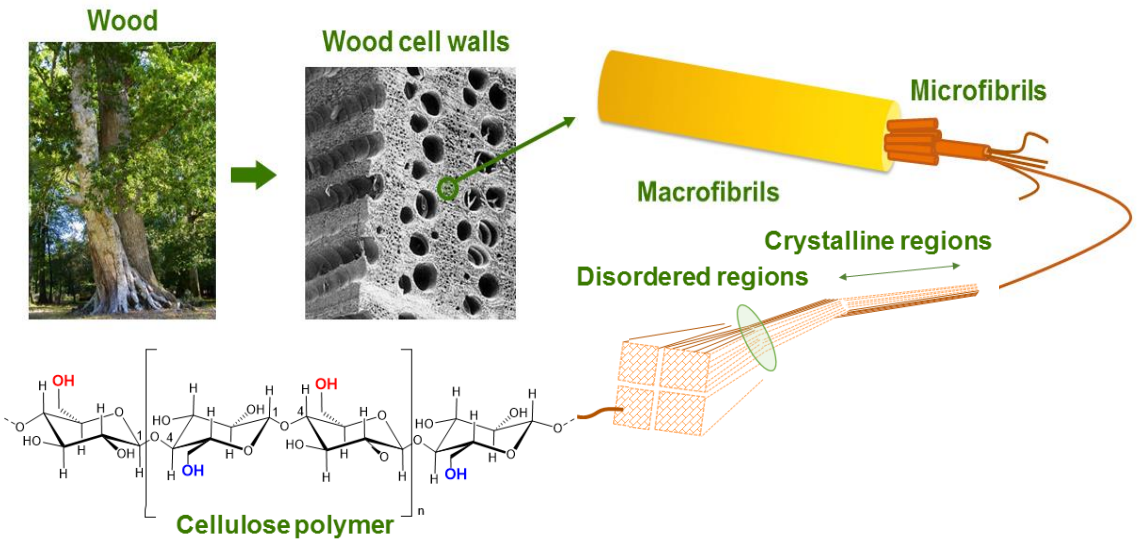

Figure 2.7: Structural hierarchy in wood (Kaushik & Moores, 2016)

Natural cellulose was discovered to have two crystalline forms: alpha cellulose (I_α) and beta cellulose (I_β) (Siqueira *et al*. 2010). In the two celluloses, their hydrogen bonds are altered: I_α has a parallel configuration, whereas I_β is anti-parallel (Habibi *et al*. 2010). I_β is found mostly in fibres such as wood, whereas I_α is predominantly found in bacterial cellulose (Boisset *et al*. 1999; Lu *et al*. 2017; Pu *et al*. 2008).

Cellulose displays high mechanical strength properties, Young modulus and crystallinity (Klemm *et al*., 2005; Morán *et al.,* 2008; Siqueira *et al*., 2010). These advantages stem from its highly organised crystalline regions, connected through hydrogen bonds and surrounded by amorphous regions linked via Van der Waals forces (George & Sabapathi, 2015; Tsoumis, 1991). These hydrogen bonds affect the properties of cellulose significantly. Crystalline cellulose is resilient to high alkali concentrations, while the amorphous structures with the weak interactional forces, are susceptible to acid hydrolysis (John & Thomas, 2008; Rusli *et al*., 2010). The hydrolysis of the amorphous area allows the isolation of mono-crystals, known as cellulose nanocrystals (CNC).

2.5.2. Hemicellulose

Hemicellulose occupies spaces between the primary and secondary wall of microfibrils and acts as a support structure for cellulose. It is related to cellulose in that they are both carbohydrates (Plants *et al*., 1984; Tsoumis, 1991), but hemicellulose contains various monosaccharaides, whereas cellulose consists entirely of β-1,4-D-glucopyranose units (Kumar *et al*., 2008; Pérez *et al*., 2002). Furthermore, hemicellulose exhibits side groups, which have shown to display low crystallinity and a DP in the rage of 30-500 (John & Thomas, 2008; Pu *et al*., 2008). The side groups of hemicellulose are sugars (D-xylose, D-mannose, D-galactose, L-arabinose and D-glucose) and acids (4-O-methyl-glucuronic, D-galacturonic and D-glucuronic acids), which are linked to the base

structure of the hemicelluloses by β -1,4- and β -1,3-glycosidic bonds (John & Thomas, 2008; Kumar *et al*., 2008; Pu *et al*., 2008).

Softwood hemicellulose units are made up of two mannose (6-carbon sugar) units known as glucomannan, arabino-glucuronoxylan and xylose. However, glucomannan is the main constituent. Hardwood hemicelluloses are predominately composed of xylose (Glucuronoxylan a 5-carbon sugar) and few mannans (Clemons, 2010; Pu *et al*., 2008). Table 2.2 shows the percentage of softwood and hardwood hemicelluloses constituents.

Wood	Hemicellulose type	% of wood
Softwoods	Galacto-glucomannan	10-15
	Arabino-glucuronoxylan	7-10
Hardwoods	Glucuronoxylan	15-30
	Glucomannan	2-5

Table 2.2: Softwood and hardwood hemicelluloses constituents (Pu *et al*., 2008)

The separation of cellulose from hemicelluloses is based on their different solubility in strong alkali solution. Hemicelluloses are soluble in alkali solutions, whereas cellulose with strong hydrogen bonds is resilient to high alkali concentrations. Various methods have shown that cellulose can be separated from hemicellulose using a 17.5 wt % sodium hydroxide solution.

2.5.3. Lignin

Lignin is a component that provides rigidity to wood, enables water conduction and reduces impregnation from outside elements (John & Thomas, 2008; Kollmann, 1968). Lignin is different from cellulose and hemicelluloses in that it is an aliphatic and aromatic hydrocarbon polymer consisting of phenylpropane units (John & Thomas, 2008). These lignin structures first develop from the natural polymerisation of p-coumaryl alcohol (p-hydroxyphenylpropanol), coniferyl alcohol (guaiacyl propanol) and sinapyl alcohol (syringyl propanol) (see Figure 2.8). The final lignin chain then consists of phenyl propionic alcohols connected to the predominately aryl-glycerol b-aryl ether base structure with C-C and aryl-ether links (Pérez *et al*., 2002).

Softwood lignin consists mainly of coniferyl alcohol, whereas hardwood lignin constituents are mostly guaiacyl and syringyl alcohols (Pérez *et al*., 2002; Pu *et al*., 2008). Lignin from softwoods

and hardwoods are generally not susceptible to acid hydrolysis, but it can be oxidised in hot alkali solutions (sodium chloride treatment or Seifert acetyl-acetone method) (MacFarlane *et al*., 1999).

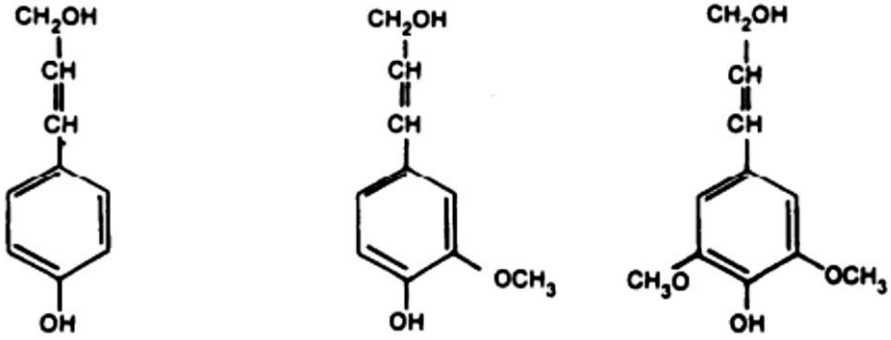

p-coumaryl alcohol coniferyl alcohol sinapyl alcohol

Figure 2.8: Precursor monomeric units of lignin (Pettersen 1984)

2.5.4. Extractives

Wood contains a collective of chemical substances called extractives. These are deposited in the cell Lumina and are not constituents of the wood structure. The elements vary from organic (oils, starch, fats and resins) to non-organic materials (calcium, silica and metals). Because they are deposits in cell walls they can easily be extracted by hot water or organic solvents, such as benzene, acetone, ether or alcohols (MacFarlane *et al*. 1999; Pettersen 1984; Tsoumis 1991).

2.6. Cellulose nanocrystals

Cellulose nanocrystals (CNC) are monocrystalline cellulose structures, which gained significant attention in recent years due to their broad set of applications. Due their high aspect ratio, rod-like, crystal structure the name cellulose nano-whiskers (CNW) is often used (Khan *et al*., 2014; Pu *et al*., 2007; Savadekar & Mhaske, 2012).

CNC particles were first isolated in the 1950s, when Ranby for the first time reported that a colloidal suspension of CNCs can be acquired from the hydrolysis of cellulose fibres using a controlled sulphuric acid-catalyst technique (Habibi *et al*., 2010). Today numerous procedures, such as mechanical digestion, enzymatic hydrolysis processing and a combination of both methods have been developed to isolate CNCs from cellulose fibres. However, acid hydrolysis remains the preferred process (Habibi *et al*., 2010; Österberg & Cranston, 2016). Although sulphuric and hydrochloric acid can both be used to isolate CNCs, a study conducted by Araki *et al*. (1998) has shown that CNCs prepared by sulphuric acid stabilize and disperse better in water

than those obtained with hydrochloric acid. The stable suspension is due to the negatively charged sulphate group that forms on the surface of the CNC during the hydrolysis process, providing an electrostatic repulsion (De Mesquita *et al*., 2010; Zhang *et al*., 2014). Figure 2.9 illustrates the sulfation of cellulose hydroxyl groups through the sulphuric acid hydrolysis process.

In cellulose fibres, the amorphous areas are more susceptible to acid hydrolysis than the crystalline areas (Kargarzadeh *et al*., 2012; Sofla *et al*., 2016). However, the breakdown of crystalline region can take place provided sufficient time, temperature or acid concentration (Sap *et al*., 2011). Studies have shown that the hydrolysis of the amorphous regions can be catalysed by increasing the free volume by improving penetration of the hydronium ions into the amorphous areas (Heath & Thielemans, 2010; Kargarzadeh *et al*., 2012). The controlled acid hydrolysis dissolves the amorphous areas, suspending the highly monocrystalline region known as CNCs (De Mesquita *et al*., 2010; Patrício *et al*., 2013).

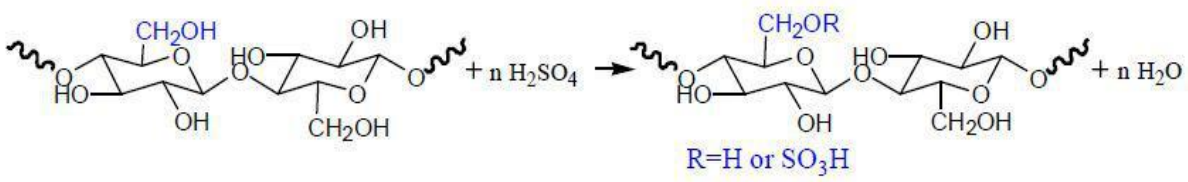

Figure 2.9: Sulfation of cellulose hydroxyl groups via sulphuric acid hydrolysis (Yuldoshov *et al*. 2016)

CNC dimensions and properties can be manipulated by the technique used to isolate them or the source of the cellulose (Dong *et al*. 1998). Studies have shown that CNC dimensions are highly influenced by hydrolysis conditions, such as reaction time, hydrolysis temperature and acid concentrations. A higher temperature, longer reaction time and strong acid concentrations lead to shorter nanocrystals (Sacui *et al*., 2014; Yu *et al*., 2013). The dimensions of CNCs are also slightly dependent on nature of the cellulose source. Cellulose sources with higher crystallinity tend to yield larger CNC dimensions. The longest CNCs isolated to date are those extracted from tunicate and bacterial cellulose. They have shown to display the highest crystallinity in the range of 95%, with an average length of 1160-2000 nm and diameter of 10-50 nm.

Many studies analysed CNC structures and dimensional characteristics with transmission electron microscopy (TEM), or atomic force microscopy (AFM) (Habibi *et al*., 2010), as illustrated in Figure 2.10. CNCs have dimensions ranging from 25 nm to several micrometres in length and 5-50 nm in diameter. However, the length and diameter of CNCs isolated from wood typically vary from 100 – 300 nm in length and 5-10 nm in diameter (Beck-Candanedo *et al*. 2005; Habibi *et al*. 2010; Morelli *et al.* 2012).

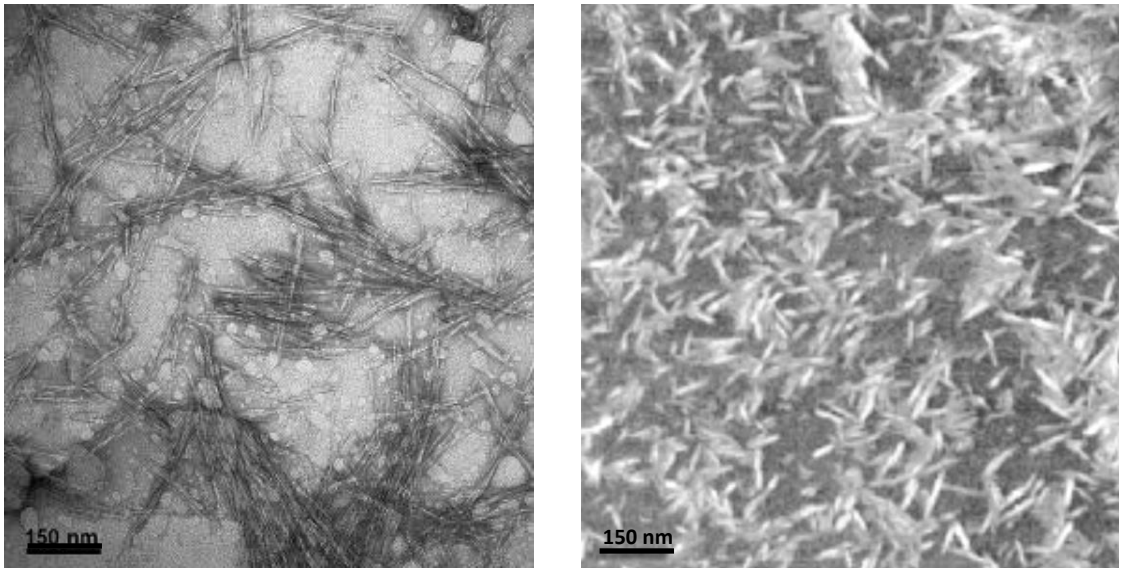

Figure 2.10: CNCs observed using TEM and AFM characterisation techniques (Petersson *et al*. 2007; Rusli *et al*. 2011)

The advantages of CNCs stem from its dimensional and compositional properties. The high aspect ratio and crystallinity of CNCs contribute towards its high mechanical properties. The tensile strength and Young's modulus (rigidity) of CNCs are estimated to be 20 GPa and between 100-180 GPa, respectively (Bondeson *et al*. 2006; Durán *et al*. 2011; Patrício *et al*. 2013; Sabo *et al*. 2016). This is comparable to some metals (aluminium and steel) and composite materials, like Kevlar (Orts *et al*., 2005). In addition to these properties, their low toxicity and large surface area also contributes to their successful use as drug blinders (Villanova *et al*., 2011), as artificial heart valves (Cherian *et al*., 2011) and as scaffolding for bone tissue (Zhou *et al*. 2013).

CNCs are flexibility, transparent, biodegradable and exhibit low thermal expansion. All these properties have lent itself towards electronic and optical development (Sabo *et al*. 2016). CNC films show low surface roughness and sheet resilience comparable to polyethylene terephthalate (PET). These properties coupled with its electrical capabilities and excellent rigidity to flexibility ratio makes CNC films suitable for flexible printed electronic parts and substrates, such as radio frequency identification (RFID) sensors, antenna tags (Sabo *et al*. 2016), light-emitting diodes, which can be used for flexible displays (Yagyu *et al*., 2015), lightweight capacitors that show significant capacitance retention (Yang *et al*. 2015) and flexible high-performance transistors (Seo *et al*., 2015; Yagyu *et al*., 2015).

These properties have also been exploited for application in electricity harvesting and storage of energy (Sabo *et al*. 2016). Degradable solar cells were developed from CNCs, based on their flexibility and near perfect transparency properties (Zhou *et al*. 2013, Fang *et al*. 2014). CNCs can be utilised as electrodes in batteries (Hu *et al*., 2013), or super capacitors *et al*. 2010) and for Li-ion battery membrane separators, as CNCs have better ionic conductivity and electrolyte wettability attributes with low thermal deformation (Leijonmarck *et al*., 2013)

More interestingly, CNCs have shown evidence of electroactive (Abas *et al*., 2014) and piezoelectric effects (Csoka *et al*., 2012), thus they can be used for actuators (Jeon *et al.*, 2010) and sensory applications in the microelectromechanical industry for robotic systems, speakers and pumps (Sabo *et al*. 2016). Another area where CNCs show promise is in the field of optoelectronics. CNCs display liquid crystal behaviour and can alter light transmittance by changing their orientation through an electrical field (Beck-Candanedo *et al*., 2005; Sabo *et al*., 2016; Teters *et al*., 2007). CNCs are therefore suitable for the manufacture of liquid crystal displays (LCD) (Sabo *et al*. 2016).

Although pure CNCs are hydrophilic, which is not desirable for any electronic devices, various studies have shown that this property can be limited by film modification with other elements and polymers, such polyimides and hexamethyldisilazane (Chinga-Carrasco *et al*. 2012; Couderc *et al*. 2009; Sabo *et al*. 2016).

Chapter 3

Experimental Work

3.1. Wood preparation

Wood from *Pinus radiata, Eucalyptus gomphocephala* and *Acacia cyclops* was received in logs with a length of approximately 30 cm. The wood was manually debarked with an axe and sharp blade. A wood chipper was initially used to reduce the size of the logs to wood chips of about 6-10 cm. The wood chips were then further reduced to a wood flower size of roughly 0.5-1 cm using a hammer mill. To acquire wood flower size in the range of 180 μm to 250 μm, the wood flower was passed through a Retch ZM100 shaker. Samples in the size range of 180 μm to 250 μm were used for all further experiments, and placed in a conditioning room until further use.

3.2. Alpha cellulose isolation

Alpha cellulose was isolated from the wood flower via the Seifert acetyl-acetone cellulose extraction method (Seifert 1960).

Wood was hydrolysed in a submerged round bottom flask with a solution ratio of 1 g wood flower to; 6 mL acetyl-acetone reagent plus (Sigma Aldrich), 2 mL 1-4-dioxane reagent plus (Sigma Aldrich) and 2 mL 32 % hydrochloric acid (Merck) for 30 minutes in a water bath at 90 °C.

After digestion the solution was transferred to a suction flask. The remaining residue in the round bottom flask was then completely rinsed with 100 mL methanol (ACE Chemicals) and also further processed through to the suction flask.

Finally, the residue in the suction flask were washed with 100 mL of each solution in the following sequence; dioxane, warm water at 80 °C, dioxane, methanol and lastly diethyl ether ACS reagent (Sigma Aldrich). Samples were then dried at 105 °C for 1 hour.

To completely remove hemicelluloses from the holo-cellulose, the hollo-cellulose was diluted at a ratio of 1 gram: 30 mL deionised water and then 2 wt% sodium hydroxide pellets (Merck) were added to the solution. The solution was then digested at 90 °C for 2 hours. Finally, the alpha cellulose was washed through a suction flask with warm water (100 °C), until residual water pH remained constant.

The process was later up-scaled using 10 g of wood with the same process ratios. Furthermore, the solvent-wood solution was stirred by a magnetic stirrer to improve process efficiency.

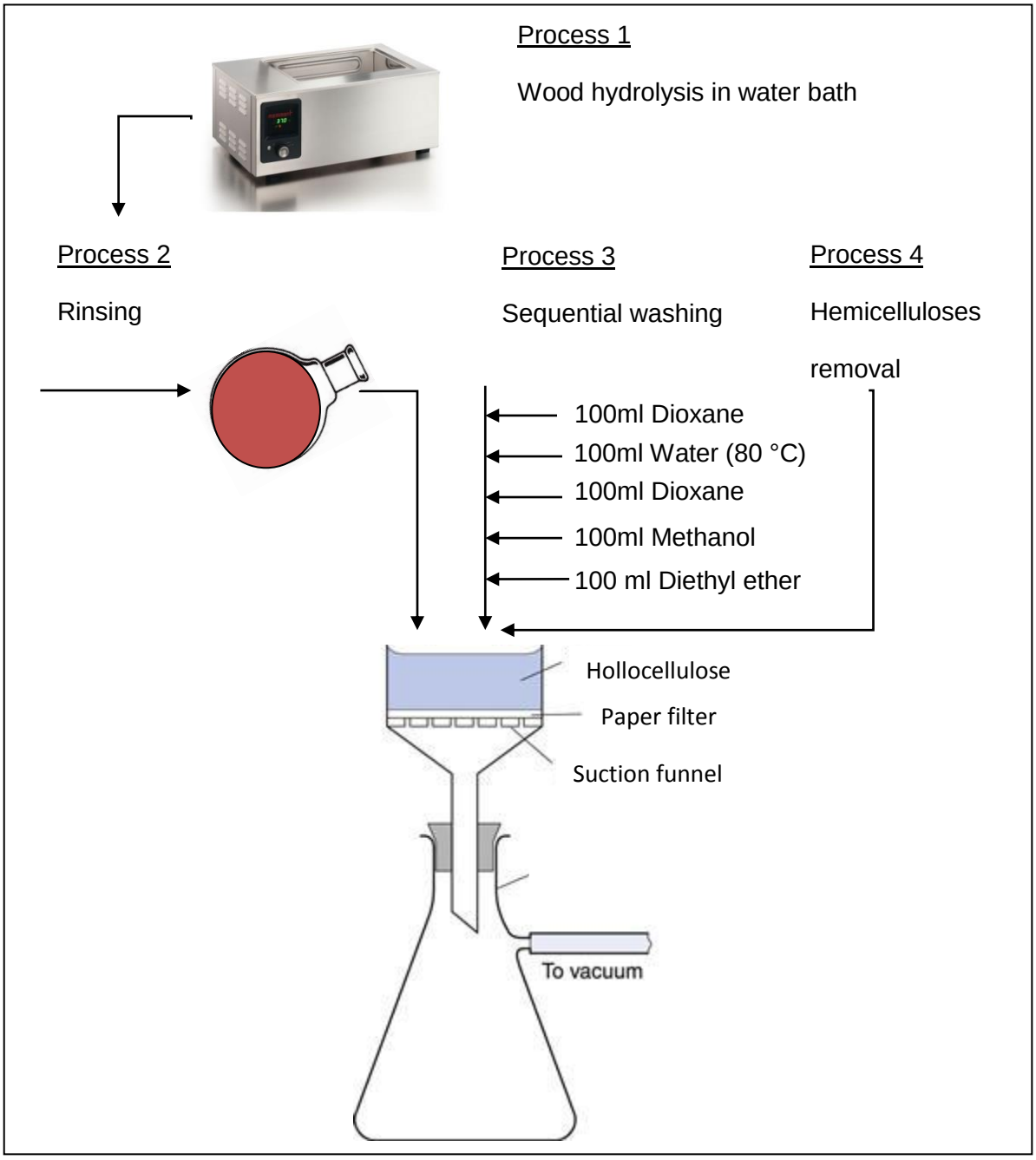

Figure 3.1: Schematic illustration of Seifert acetyl-acetone alpha cellulose isolation

Commercial α-cellulose was obtained from Sigma Aldrich. It was not disclosed how it was processed or from what source(s) it was isolated.

3.3. Preparation of Cellulose nanocrystals (CNCs) through acid hydrolysis

CNCs in this study were isolated using a slightly altered technique of Bonderson *et al*. (2006). The authors optimally extracted CNCs from microcrystalline cellulose utilising a 64 wt% acid hydrolysis solution.

In this study a solution consisting of deionised water, to swell the amorphous areas, and wood powder was mixed together in a ratio of 1 gram: 20 mL respectively.

The solution and sulphuric acid (Merck) in ratio of 1:1 mL, respectively were placed separately in an ice bath. The solution was slowly stirred at 200 rpm for 30 minutes, which provided uniform cooling. This prevented an increase to critical temperature that could cause cross-linking of the cellulose during the following reaction.

After 30 minutes the solution was then vigorously stirred at around 900 rpm, while the sulphuric acid was dripped into the solution at 1 mL sulphuric acid per minute over 60 minutes. Subsequently the ice bath was replaced with an oil bath and the reaction temperature was held at 50 °C for 90 minutes.

Afterwards the suspension was distributed equally into four centrifuge tubes. The hydrolysis reaction was cooled and quenched by diluting the suspension in the centrifuge tubes, tenfold with deionised water. CNCs and excess acid were separated from the dissolved amorphous regions during the centrifugation process (explained below) and the remaining trace amounts of acid that could not be extracted by centrifugation were neutralised via dialysis after centrifugation.

Deionised water, used as the exchange medium for the supernatant during centrifugation, and the suspension were shaken to mix completely. The dissolved suspension was subsequently centrifuged at 5000 rpm for 5 minutes and these two steps were repeated until the supernatant appeared turbid. Once the supernatant became turbid the suspension was centrifuged twice more, to ensure that the turbid layer contained only CNCs. Centrifugation and collection of turbid suspension continued until the supernatant became clear again.

The gathered turbid solution containing the CNCs was dialysed until a constant pH of 6.5, which ensured the removal of any trace amounts of acid that may have remained after centrifugation.

Freeze drying was used to obtain solid CNC’s powders.

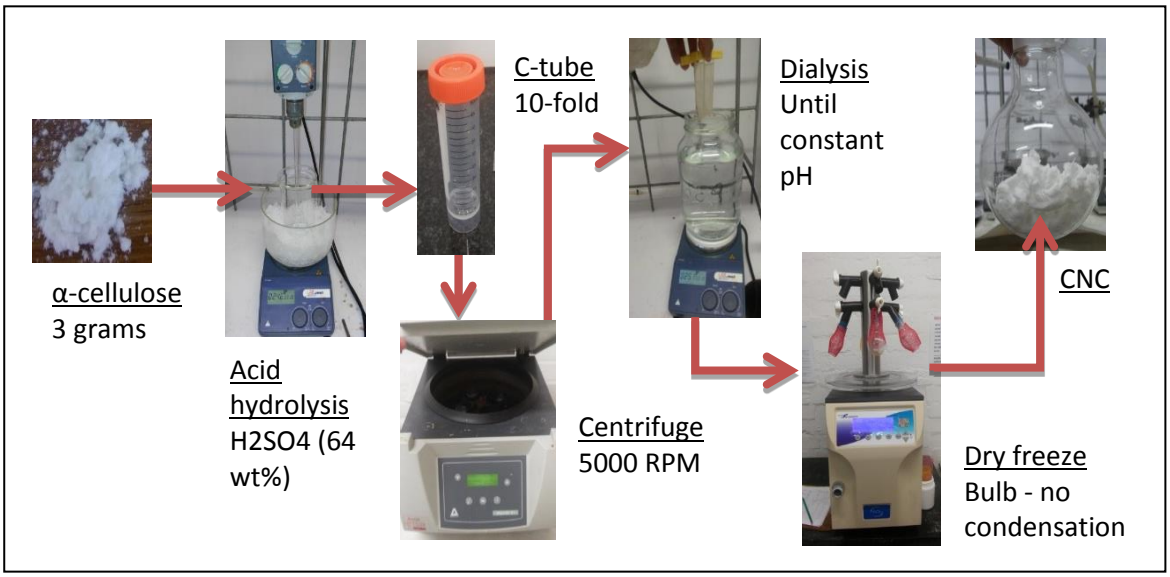

Figure 3.2: Schematic illustration for acid hydrolysis CNC synthesis process

3.4. Characterisation of alpha-cellulose and CNCs

3.4.1. X-ray diffraction (XRD)

X-ray diffraction (XRD) is one of the most important non-destructive analytical techniques used to investigate solid materials. This method provides information on cell unit dimensions, which is primarily used for the phase identification of crystalline materials, chemical composition and physical properties (Reventós *et al* 1912)

Crystalline materials have a very specific x-ray diffraction pattern. The crystallinity of a material is determined through Bragg's Law ($n\lambda = 2d\sin\theta$), which correlates the wavelengths of the diffracted x-rays to the scatter angle (θ) and lattice spacing (d) of material (see figure 3.3) (Reventós *et al*., 1912). To account for all potential diffraction angles, samples are scanned through a range of two-theta (2θ) with monochromatic x-rays, which are produced by a cathode ray tube and directed at the sample.

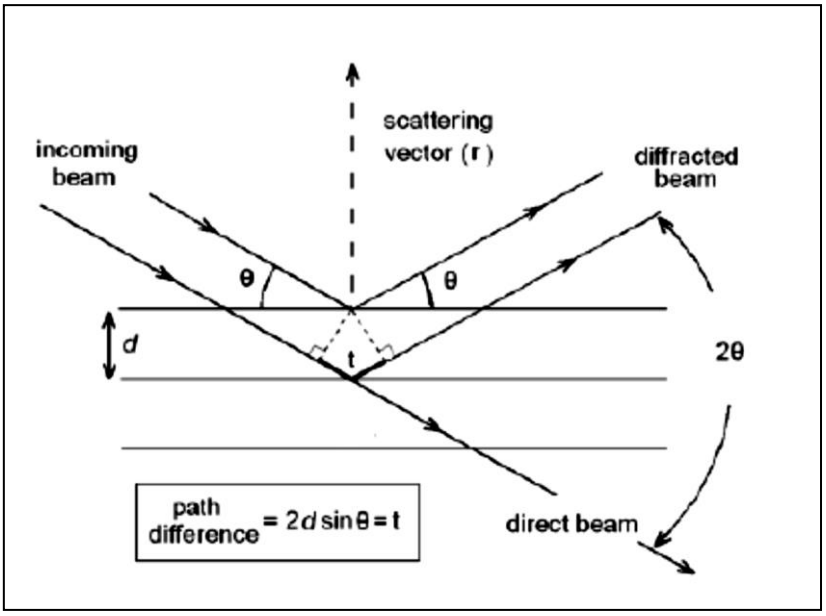

Figure 3.3: Illustration of Bragg's law (Reventós *et al*., 1912)

The crystallinity of cellulose and CNCs was determined from XRD spectra by using Segal's method (Segal *et al*., 1959). According Segal's empirical equation, the crystallinity X_c can be established using the variables I_{002} and $I_{amorphous}$ (see Equation 4.1). Where I_{002} is the maximum crystalline lattice peak intensity of diffraction and $I_{amorphous}$ is the minimum amorphous lattice intensity between I_{110} and I_{200} at a 2θ angles (see figure 4.2).

$$X_c = \frac{I_{200} - I_{amorphus}}{I_{200}} \times 100\% \quad (3.1)$$

The crystallinity of alpha cellulose and CNCs was determined by XRD (Bruker AXS D8 advanced diffractometer) at iThemba LABS. All samples were scanned at room temperature with CuKα filtered radiation. CNC and alpha cellulose powders were first compressed into disks before analysis. Samples were scanned at 2θ diffraction angles ranging of 6.0° to 65.0° in step increments of 0.034°.

3.4.2. Fourier transform infrared spectroscopy (FTIR)

FTIR is an effective analytical technique used to identify functional groups and characterise chemical structures in samples (Morán *et al*. 2008). IR absorption for particular functional groups and bonds occur at different wavelengths, making this technique suitable to identify these functional groups (Ylmén *et al*., 2009).

FTIR is one of the most preferred and effective analytical methods used to determine the removal of impurities, such as lignin and hemicelluloses form wood, confirming the purity of cellulose and CNCs (Morán *et al*. 2008; Morelli *et al*. 2012).

FTIR data was collected using a Thermo Fisher iS10 ATR-FTIR instrument in Attenuated Total Reflection (ART) mode, to obtain information of the chemical composition of the samples and ensure that no hemi-cellulose was present. The data were recorded in 32 scans in a wave length range between 650 cm^{-1} and 4000 cm^{-1}at resolution of 4 cm^{-1}.

3.4.3. Transmission electron microscopy (TEM)

TEM is a very important analytical technique in dimensional and structural characterization of nanoparticles. It is also used to verifying the identity of chemical and electron structures in singular nano-structures such as CNCs (Wang 2000).

TEM utilises an electron beam to interact with the material. The change in energy levels is directly proportional to the particle size, This in turn influences the emission of photons with a unique wavelength. These waves that pass through the particle are then captured by optoelectronics (Wang 2000).

The use of TEM as a structural analytical tool to structurally characterize of CNCs from various sources have been well documented (see figure 3.4) (Kaushik *et al*. 2015; Kaushik & Moores 2016; Rusli *et al*. 2010; Sofla *et al*. 2016)

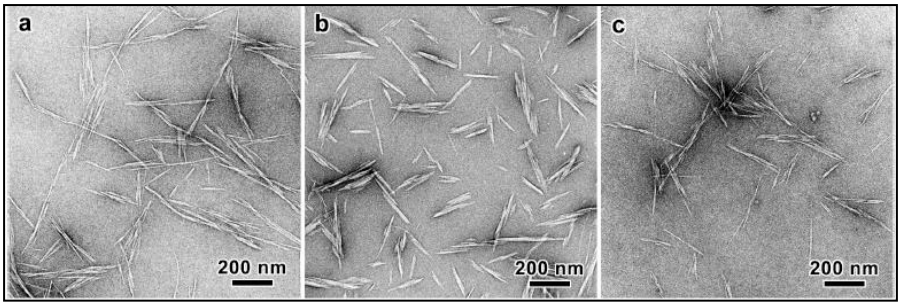

Figure 3.4: CNC TEM images from various sources: a) wood, b) cotton, c) bamboo (Kaushik *et al*. 2015)

Visual characterization of CNC length was conducted by STEM analysis. All sample images of lower and higher magnifications were taken with a LEO 912 EM STEM instrument. 0.001 wt% diluted CNCs were transferred onto carbon coated TEM grids, stained with uranyl acetate and

were allowed to dry at room temperature. This technique, however allowed the length determination of only a few CNCs.

3.4.4. Atomic force microscopy (AFM)

AFM is an analytical technique commonly used to provide three-dimensional topography data at nanometer levels (Habibi *et al*., 2010). However studies have also shown that it is useful in quantifying structural interactions and chemical properties, such as rigidity (elastic modulus) of a material (George & Sabapathi, 2015; Lahiji *et al*., 2010).

As shown in figure 3.5, AFM uses a cantilever with a sharp tip to survey the surface of a sample. As the tip scans the sample repulsion forces cause the cantilever to deflect away from the sample surface and this deflection is recorded by the change of position of a laser beam, reflecting off the flat top of the cantilever. A position sensor then tracks these changes plotting it as a colour coded topography image (Meyer & Amer 1988).

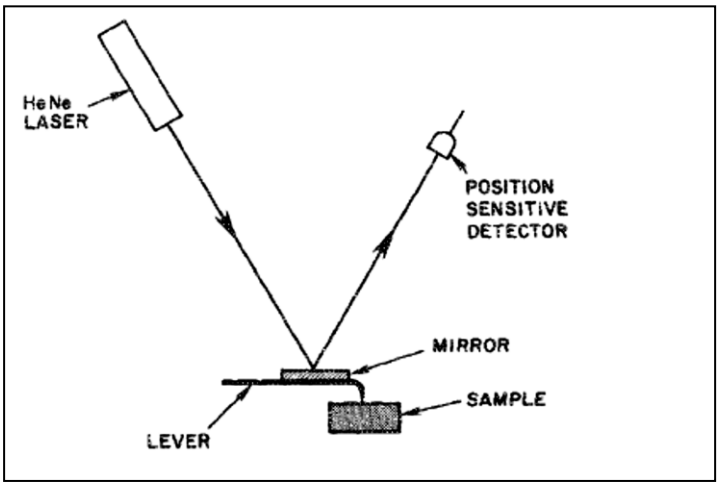

Figure 3.5: Schematic Illustration of AFM cantilever deflection and sample topography detection (Meyer and Amer 1988).

Three-dimensional characterization of CNCs to obtain the length, as well as the diameter was conducted on an EasyScan 2 AFM instrument from Nanosurf Switzerland. A contact Si cantilever from Nanoworld was used with a spring constant of 0.2 N/m. CNCs were diluted to 0.001 wt% and 0.0001 wt% in distilled water and cast on a freshly cleaved mica surface. AFM images were acquired after the samples were dried and the CNCs adhered firmly to the mica surface. An average of 20 CNCs were analysed per wood species.

3.4.5. Dynamic light scattering (DLS)

DLS is a frequently utilised technique for quantifying the size and size distribution of nano-materials in a colloidal suspensions (Hoo *et al*. 2008; Pecora 2000)

Particles suspended in liquid experience random Brownian motion and light that is passed though the suspension is scattered off the particles. The refractive indices are continually changing due this motion, which is detected by a sensor, which uses the Stokes–Einstein equation to determine the size distribution of the suspension (Hoo *et al*. 2008)

The length distribution of CNCs on a larger scale was determined via DLS in a Zetarsizer (R) Nano-ZS90 size analyser from Malvern Instruments. CNC samples were diluted in water between 0.001-0.0003 wt% and then sonicated at 50 KHz for 1 minute.

3.4.6. Differential Scanning Calorimetry (DSC)

DSC provides information on physical and chemical property changes of a material as a function of increasing constant temperature (du Toit, 2013).

A sample is weighed and placed in an aluminium pan. The pan is placed onto a balance scale with another empty reference pan. Heating takes place in a nitrogen atmosphere. As degradation starts the balance of the two pans begin to destabilise and this is relayed to a sensor which then quantifies the above information.

Thermal degradation of CNCs was analysed by a TA Q100 differential calorimeter instrument. About 3 mg were first cooled to 0 °C and then heated to 350 °C with a heating rate of 10 °C/min in an inert nitrogen atmosphere.

Chapter 4

Results and discussion

4.1. Introduction

Cellulose nanocrystals were synthesised from four cellulose sources, namely acacia, eucalyptus, pine and commercial cellulose. This was done in order to determine if CNC properties vary between wood species and if CNCs isolated from invasive South African hardwoods compare to CNCs synthesised from commercial cellulose. Cellulose and CNCs were characterised by means of Fourier Transform Infrared Spectroscopy (FTIR), X-ray diffraction (XRD), transmission electron microscopy (TEM), dynamic light scattering (DLS), differential scanning calorimetry (DSC) and atomic force microscopy (AFM).

4.2. Fourier transform infrared (FTIR) spectroscopy

To isolate pure cellulose, lignin and hemicelluloses need to be completely removed from the wood. The presence of lignin can be verified by C=C bonds of aromatic rings, which appear in the absorption range between 1460 and 1600 cm^{-1} (Morán *et al* 2008). The presence of hemicellulose can be determined through C=O bonds in the absorption range around 1730 cm^{-1} (Morelli *et al*., 2012). The FTIR spectra of wood, α-cellulose and CNCs synthesised from the three invasive wood species are displayed in Figure 4.1. The spectra show that the Seifert acetyl-acetone and sodium hydroxide methods were successful in removing lignin and hemicelluloses, thus producing the required α-cellulose standard to synthesise CNCs.

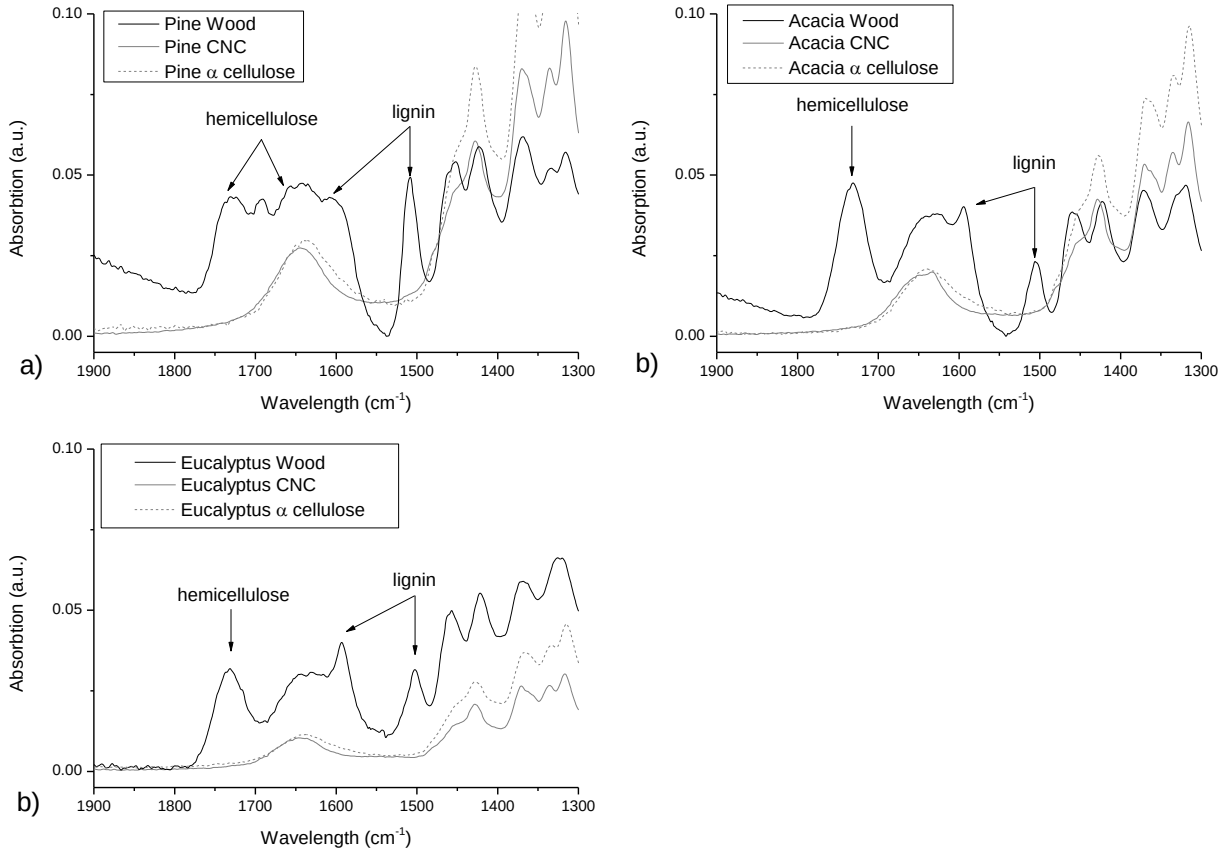

Figure 4.1: FTIR spectra of wood, α-cellulose and CNCs for a) pine, b) acacia and c) eucalyptus

4.3. X-ray diffraction (XRD)

The XRD spectra of α-cellulose and CNC crystallinity for the various wood species are displayed in Figure 4.2.

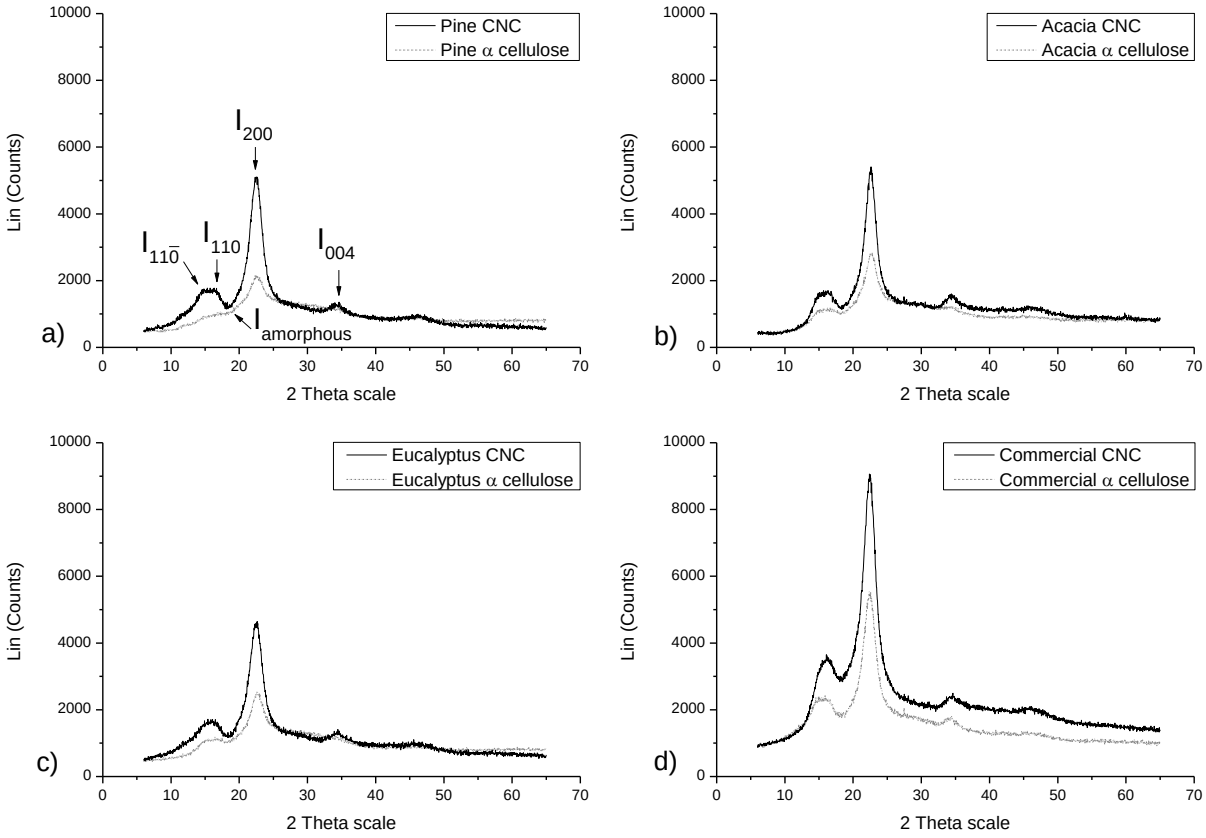

Figure 4.2: XRD spectra of α-cellulose and CNCs from a) pine, b) acacia, c) eucalyptus and d) commercial cellulose

The peaks of $I_{11\bar{0}}$, I_{110}, I_{002} and I_{004} are defining characteristics of cellulose I (Gaspar *et al*., 2014; Morelli *et al*., 2012; Sofla *et al*., 2016). The indices, $I_{11\bar{0}}$, I_{110} and I_{200} observed around 2θ = 14°, 17° and 22.7° respectively are peaks perpendicular to the fibre axis. These peaks are caused by crystallographic planes of monoclinic cellulose I (Gaspar *et al*., 2014; Yu *et al*., 2013).The I_{004} index, which appears at approximately 35°, is a peak parallel to the fibre axis (Grange, 2015).

Compared with α-cellulose, CNCs display broader and higher intensity peaks ($I_{11\bar{0}}$, I_{110}, I_{002} and I_{004}). This confirms that noncellulosic polysaccharides and amorphous regions were effectively

removed from the crystalline areas during the acid hydrolysis process (Yu *et al*., 2013). Thus, CNCs display higher crystallinity than α-cellulose as shown in Table 4.1.

CNCs isolated from acacia, eucalyptus, pine and commercial α-cellulose display a crystallinity between 72 and 79%. Other studies utilising acid hydrolysis to prepare CNCs from wood documented a crystallinity in the same range (Chen *et al*. 2011; Cherian *et al*. 2010; Kargarzadeh *et al*. 2012).

Source	Wood (Xc)	α-cellulose (Xc)	CNC (Xc)
Acacia	55%	66%	79%
Eucalyptus	49%	61%	75%
Pine	54%	60%	77%
Commercial	-----	68%	72%

Table 4.1**:** Crystallinity of α-cellulose and CNCs from the various sources

The crystallinity of the untreated wood fibres is 55, 49 and 54 % for acacia, eucalyptus and pine, respectively. The difference between the wood species can be explained by the fact that the species exhibits different amounts of hemicelluloses, lignin and cellulose.

The crystallinity of the purified α-cellulose increased to 66, 61 and 57 % for acacia, eucalyptus and pine, respectively. This increase in crystallinity results predominantly from the removal of hemicelluloses and lignin constituents that form part of amorphous regions (Chen *et al*. 2011). Commercial cellulose exhibited the highest crystallinity (68 %) compared to the α-cellulose samples isolated with Seifert acetyl-acetone method. This could be a result of more efficient α-cellulose extraction techniques used compared to the Seifert acetyl-acetone process used in this study.

CNCs isolated from acacia displayed the highest crystallinity with 79 %, followed by pine (77 %), eucalyptus (75 %) and commercial CNCs showing the lowest (72 %). The large increase in crystallinity from acacia, eucalyptus and pine demonstrated that hydrolysis predominately took place in amorphous regions. This has been reported in depth by many authors (Bondeson *et al*.,

2006; Cherian *et al*., 2010; De Mesquita *et al*., 2010; Kargarzadeh *et al*., 2012). The differences in crystallinity could be due to variation in α-cellulose content between the wood species. CNCs isolated from commercial α-cellulose displayed only a slight change in crystallinity from 68 % to 72 %. This could possibly be due to commercial α-cellulose consisting of much smaller particles (45 µm-180 µm) compared to the larger cellulose particles obtained from milling acacia, eucalyptus and pine (180 µm-250 µm). Smaller particles are more susceptible to degradation in high acidic concentrations, thus the faster degradation of smaller amorphous areas could have led to early exposure of crystalline regions to the high acidic conditions. Literature has shown that crystalline regions are also at risk to degradation if time, temperature and high enough acidic concentrations are high enough (Bondeson *et al*. 2006). Under these harsh conditions, CNC dimensions will be reduced, resulting in lower crystallinity. Therefore, CNCs made from commercial cellulose could have benefited from shorter hydrolysis times.

Crystallinity is one of the most important CNC properties, as it provides mechanical strength, thermal stability and acid resistant properties. Therefore, higher crystallinity is desirable for application, such as bulletproof CNC reinforced materials, heart valves and electrical devices, like capacitors and batteries. CNCs with lower crystallinity could be used in the medical field for products, such as drug capsules and binders, which do not require materials of high strengths.

The softwood and hardwood CNCs analysed in this study compare well to CNCs made from commercial cellulose and exhibit no significant differences in crystallinity. Therefore, they can be expected to show similar mechanical properties.

4.4. Yield

Cellulose

The yield of α-cellulose was calculated as the mass percentage that remained after Seifert acetyl-acetone and sodium hydroxide hydrolysis. The average yield is listed Table 4.2. The same index indicates significant differences with $p<0.05$.

Source	Yield (%)
Acacia ^{abc}	40,1 ± 0.9%
Eucalyptus ^{bac}	37,2 ± 1.1%
Pine ^{cab}	43,3 ± 0.5%

Table 4.2: Average α-cellulose yield for acacia, eucalyptus and pine

Pine displayed the highest yield (43.3±0.5%) followed by acacia (40.1±0.9%) and eucalyptus (37.2±1.1%). All sample yields were found to be significantly different from one another.

CNCs

The method used in this study to calculate CNC yield was adopted from Bondeson, Mathew & Oksman (2006).The yield is calculated as a percentage of the initial weight after the hydrolysis of α-cellulose. Table 4.3 shows the yield for acacia, eucalyptus, pine and CNCs from commercial cellulose.

Source	Yield (%)
Acacia	34,5 ± 4.3%
Eucalyptus	24,0 ± 7.2%
Pine	26,9 ± 2.8%
Commercial	31.0 ± 5.0%

Table 4.3: CNC yield for acacia, eucalyptus and pine and commercial cellulose

The CNC yield ranged from 24% to 34.5% depending on the cellulose source. Acacia had the best average yield of 34.5±4.2% and eucalyptus the lowest with 24±7.2%. Eucalyptus also showed the highest standard deviation, whereas pine exhibited the lowest. Fall *et al*. (2014) synthesised CNCs from pine and acacia via enzymes and reported yields of 30% and 32%, respectively, which is similar to the yields obtained in this study. According to Bondeson *et al*. (2006), a CNC yield between 25 and 45 wt% is considered reasonable. Therefore, eucalyptus is the only cellulose source exhibiting a marginally unsatisfactory CNC yield. There are no significant differences in yield between the various CNC sources ($p>0.05$).

Pine and eucalyptus display lower yields compared to acacia and CNCs from commercial cellulose. One of the factors that affects the CNC yield, which has been reported by many authors, is the charge density of the wood pulp (Fall *et al*. 2014; Fall *et al*. 2011; Iwamoto *et al*. 2010). These authors have shown that a higher charge density leads to a more effective separation of cellulose, resulting in higher CNC yields. No significant difference was found between hard- and softwoods, as eucalyptus and pine showed similar yields, but acacia had a significantly higher yield than both pine and eucalyptus.

4.5. Transmission electron microscopy (TEM)

TEM was used to confirm that CNCs were successfully isolated by acid hydrolysis and that they had a homogenous size distribution. Figure 4.3 displays the TEM images of CNCs isolated from commercial α-cellulose as an example.

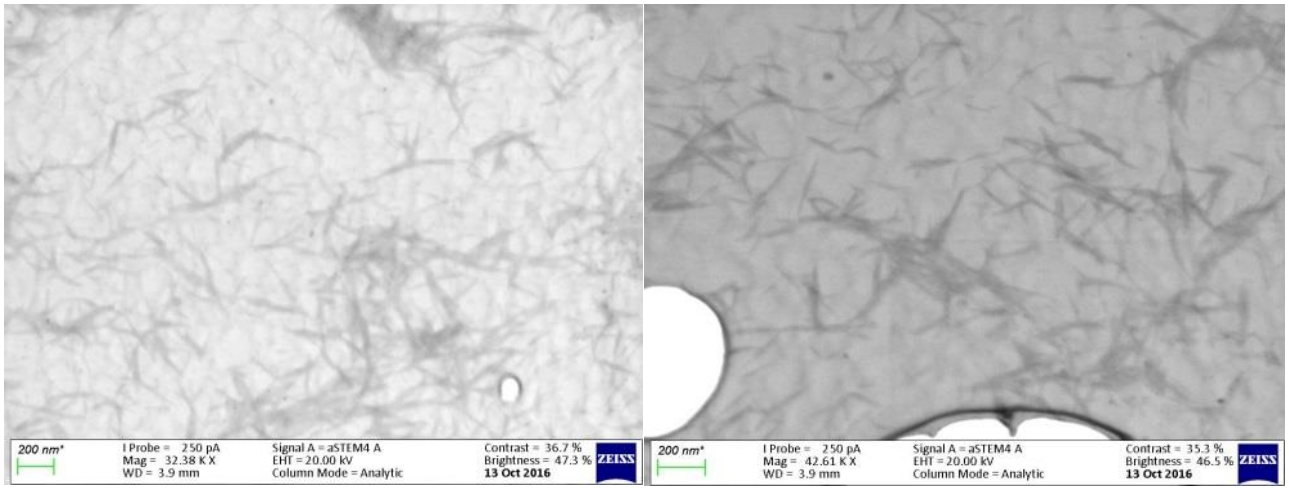

Figure 4.3: Shows TEM images of CNCs isolated from commercial α-cellulose

Table 4.4 summaries the twenty four TEM measurements and standard deviations taken from each CNC species. The same index indicates significant differences with $p<0.05$.

Source	Average length (nm)	Number of particles measured (n)
Acacia [a]	131 ±28	25
Eucalyptus [ba]	179 ±55	30
Pine [ca]	176 ±47	28
Commercial [da]	183 ±55	24

Table 4.4**:** Average particle length and standard deviation of CNCs isolated from acacia, eucalyptus, pine and commercial cellulose.

CNCs from commercial cellulose have longest CNCs with 183 nm, followed by eucalyptus (179 nm) and pine (176 nm), however they are not significantly different ($p>0.05$). On the other hand acacia is significantly in smaller length (131 nm) compared to eucalyptus, pine and commercial

CNCs ($p<0.05$). These values are comparable to results from Morelli *et al*. (2012) and Kargarzadeh *et al*. (2012), who reported CNC length between 124±45 and 176±68 nm.

The dimensions of the CNCs analysed in this study comply with the ISO/TS 20477:2017 standard (ISO/TC229, 2017), which defines the various types of nano-cellulose. According to this Standard a CNC is defined as particle with at least one dimension in the nano-scale range (100 nm or below), which is derived from a cellulose source whether it be plant or animal based.

No difference in CNC dimensions was found between hardwoods and softwoods. However, CNCs from acacia were significantly shorter than all others. Thus, acacia CNC could be used in applications, such as nanofilters, medical binders and capsules, which require smaller particle, whereas larger CNCs would be more suited for reinforcements in nanocomposites, or flexible displays and electrodes.

4.6. Dynamic light scattering (DLS)

Dynamic light scattering is used to determine the lengths of numerous CNCs in one batch and provide information as a distribution of particles sizes. Twenty-five scans were conducted on each sample and the average size (length) distribution is displayed in Figure 4.4 on a logarithmic scale. It shows that more than 90 % of the particles are in a range between 100 and 1200 nm.

Also shown in Figure 4.4, pine and acacia both exhibit narrower size distributions than eucalyptus and CNCs from commercial cellulose. A narrow size distribution indicates that particles are homogeneous in size with small variations, whereas a wider distribution indicates a larger standard deviation.

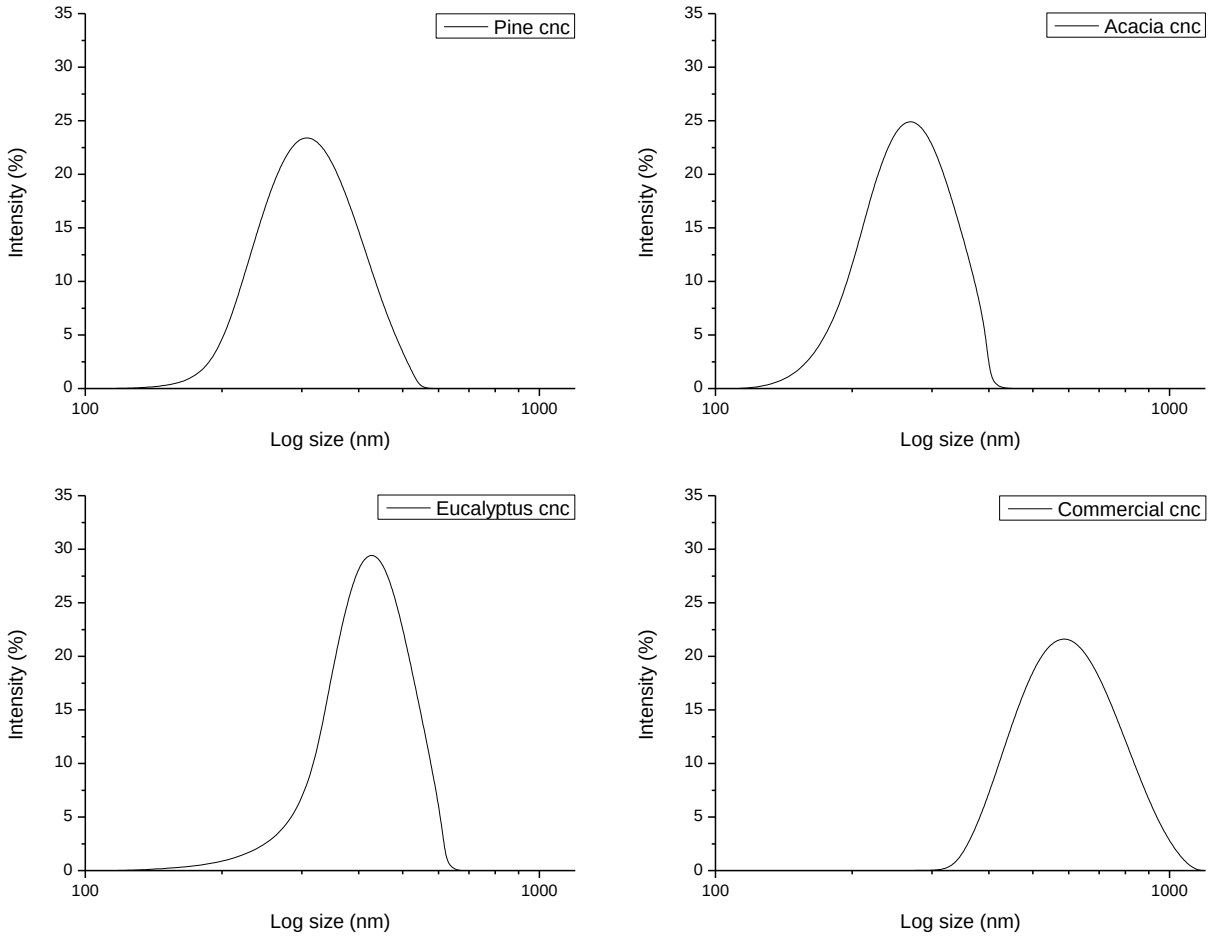

Figure 4.4: Log size distribution of CNCs isolated from a) pine, b) acacia, c) eucalyptus and d) commercial cellulose.

The average particle size of CNCs isolated from acacia, eucalyptus, pine and commercial cellulose is shown in Table 4.5.

Source	Average length (nm)
Acacia	295±15
Eucalyptus	382±58
Pine	311±32
Commercial	549±44

Table 4.5**:** Average particle length and standard deviation of CNCs isolated from acacia, eucalyptus, pine and commercial cellulose

CNCs isolated from commercial cellulose are the largest in size (549±44 nm), followed by eucalyptus (382±58 nm) – which also displays the highest variation of 15 %, pine (311±32 nm) and acacia. Acacia with an average length of 295±15 nm showed the lowest standard deviation of roughly 5 %. CNCs produced from commercial α-cellulose are similar in lengths to CNCs extracted from other cellulose sources, such as tunicate and bacterial cellulose, that have the potential to range above 500 nm in length. Larger CNCs could potentially be used in LCDs, transparent high strength films and in the electrical industry as magnetic actuators.

CNCs from acacia, eucalyptus and pine had length dimensions between 295 and 382 nm, which is significantly shorter that CNCs isolated from commercial cellulose (549 nm). The isolation technique and source of the commercial α-cellulose is unknown and could potentially have a significant influence on CNC proportions.

4.7. Atomic force microscopy (AFM)

Atomic force microscopy was used to image individual CNC particles to confirm dimensions obtained by DLS, TEM and to determine the diameters of CNCs. Since DLS determines the particle size of a large number of particles, it is possible that some of them were particle agglomerates, or shorter particles. Therefore, AFM was used to confirm the dimensions, on a few individual CNCs. Furthermore, AFM allows the separate determination of length and diameter, which is not possible through DLS. Figure 4.5 displays AFM images of CNCs isolated from eucalyptus.

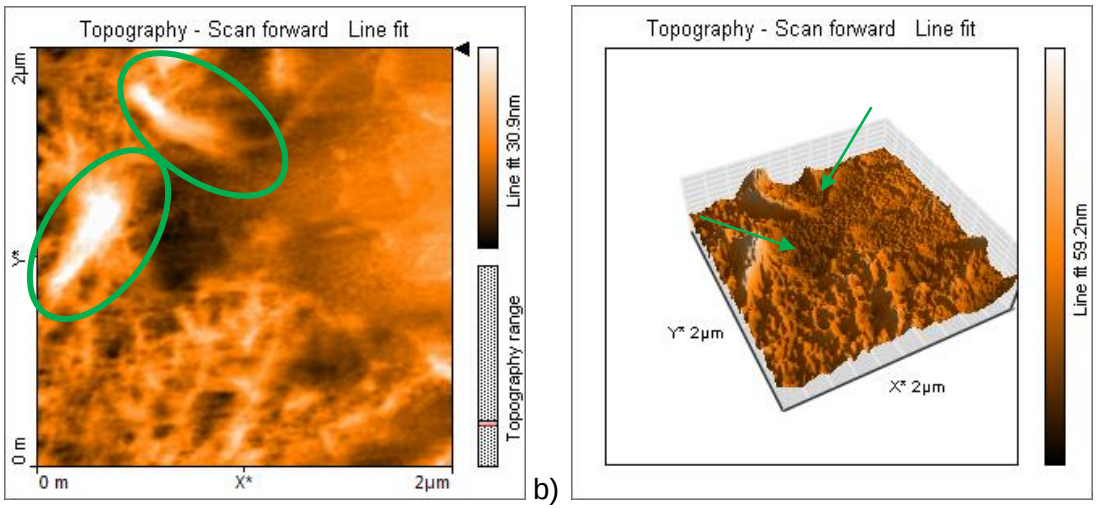

Figure 4.5: AFM images of CNCs from eucalyptus, a) topography and b) 3D image.

Ten individual CNCs that were not part of an agglomerate, were located from each sample to determine the length and diameter listed in Table 4.6.

Source	Length (nm)	Diameter (nm)	Number of particles measured (n)
Acacia	252± 90	5 ±2	14
Eucalyptus	377±126	5 ±1	16
Pine	250±111	3 ±1	11
Commercial	333±287	4 ±3	23

Table 4.6**:** Average length and diameter of CNCs with standard deviation

Acacia and eucalyptus have the same average diameter of 5 nm, however acacia is seen the exhibit a larger variation in size. Commercial CNCs displayed an average diameter of 4 nm with the largest variation in size, where as those isolated from pine showed the smallest diameter of 3 nm. CNCs analysed in this study exhibits a similar diameter between 3-5 nm to CNCs analysed by Habibi *et al*. (2010) and Morelli *et al*.(2012).

CNCs from eucalyptus yielded the longest CNCs, with an average length of 377±126 nm, followed by CNCs from commercial cellulose (333±287 nm), acacia (252± 90 nm) and pine (250±111 nm). CNCs from commercial cellulose however showed the largest variation of 86 % of the average length, which is significantly different from pine (44 %), acacia (35 %) and eucalyptus (33 %).

Although there are differences in average lengths and standard deviations, all CNC dimensions analysed by AFM were not significantly different from one another ($p>0.05$).

Table 4.7 compares the dimensions obtained by TEM, DLS and AFM

Source	TEM (nm)	DLS (nm)	AFM (nm)
Acacia	131 ±28	295 ±15	252 ±90
Eucalyptus	179 ±55	382 ±58	377 ±126
Pine	176 ±47	311 ±32	250 ±111
Commercial	183 ±55	549 ±44	333 ±287

Table 4.7**:** Comparison of dimensional analytical techniques

TEM analysis yielded the lowest length values (131-183 nm), compared to DLS (295-549 nm) and AFM (250-377 nm). With regards to DLS and AFM lengths, the obtained values are similar. The average length determined by DLS and AFM for eucalyptus, acacia, pine and CNCs from commercial cellulose are in some cases more than double or even triple the lengths determined by TEM. The average length determined by AFM had the highest standard deviations, ranging between 33-86 %. This can be explained by the small sample size of CNCs analysed by AFM. Standard deviations of values obtained by TEM and DLS were similar in value.

The reason for the differences between TEM, DLS and AFM is largely due to the amount of CNC analysed in each method. TEM and AFM both analyse individual CNC particles, with TEM allowing the analysis of a larger variety of particles, because the image size (and with that particle number) is larger. In the TEM images, all particle dimensions were determined and reported as average, whereas for AFM analysis only a few perfect CNCs where selected for analysis. Furthermore, the AFM image is always a product of the particle and AFM tip dimensions, resulting on slightly larger values. The low sample number in the AFM analysis resulted in much larger standard deviations than TEM and DLS. DLS on the other hand displayed the lowest standard deviation because it is able to analyse much larger amounts of CNCs.

4.8. Differential Scanning Calorimetry (DSC)

Thermal stability is an important aspect to consider when determining a suitable application for CNCs. For CNCs to be used in the electrical field, for example, as capacitor it has to be thermally stable within a range between -40°C and 125°C (du Toit, 2013; Dubilier, 2011).

Studies have shown that the DSC peaks shows the temperature of thermal degradation, as no melting was observed in CNCs (Mandal & Chakrabarty, 2011). Figure 4.6 displays thermal degradation curves obtained by DSC for pine, acacia, eucalyptus and CNCs from commercial cellulose. Pine, acacia and eucalyptus exhibit narrower peaks than commercial CNCs, which means that commercial CNCs have a much wider range of thermal degradation, compared to the other CNC sources.

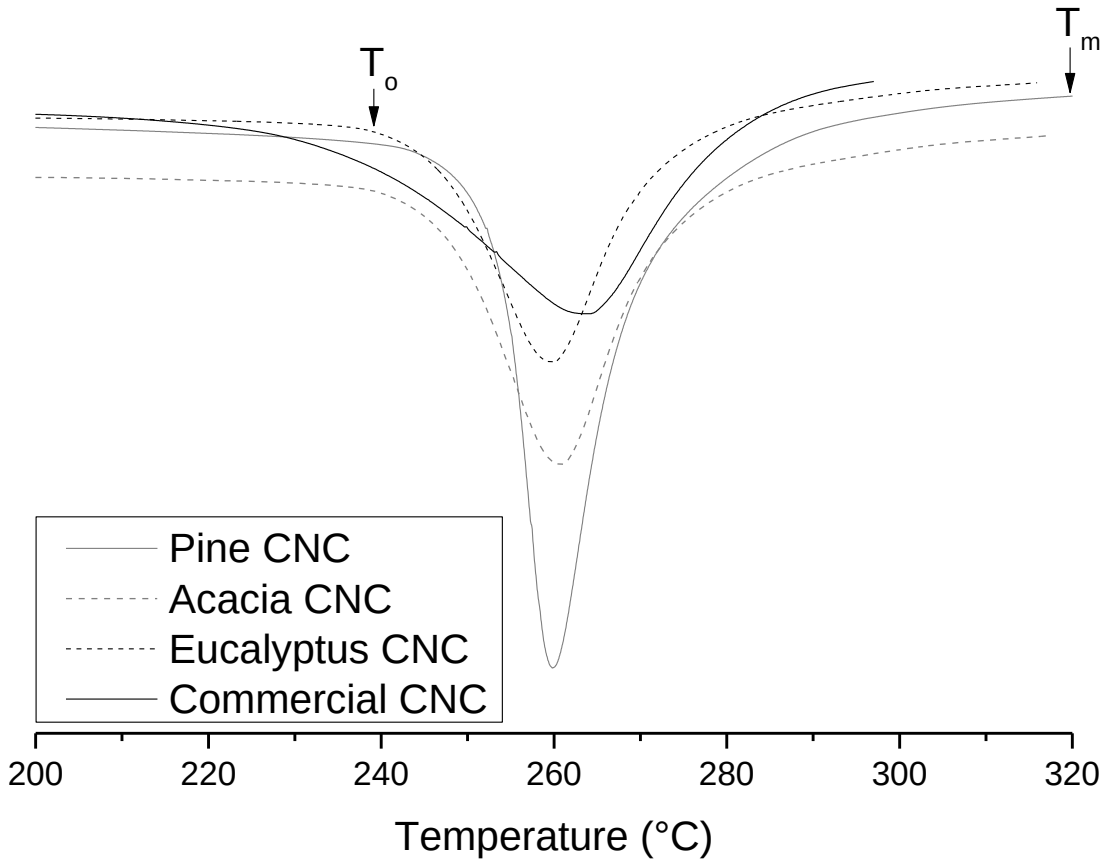

Figure 4.6: DSC curves of pine, acacia, eucalyptus and commercial CNCs

Table 4.8 shows the onset (T_0) and maximum (T_m) degradation temperatures at which CNCs from acacia, eucalyptus, pine and commercial cellulose degrade. T_0 is the point at which the CNCs begin to degrade and T_m is the temperature, at which all the CNCs have degraded.

Source	T_0 (°C)	T_m (°C)
Acacia	237	316
Eucalyptus	230	315
Pine	242	320
Commercial	210	300

Table 4.8**:** Onset and degradation temperature of CNCs

Pine showed the highest maximum degradation temperature, while CNCs from commercial cellulose displayed the lowest onset degradation temperature compared to the other CNC samples. However, all CNCs are not significantly different from one another in terms of thermal

resilience. The values displayed in Table 4.8, which range from 210 to 242 °C for the onset and 300 to 320 °C for the maximum degradation temperatures are similar to those reported by Morelli *et al*. (2012).

Chapter 5

Conclusion and future recommendations

5.1. Conclusion

CNCs were successfully isolated from acacia, eucalyptus, pine and commercial α-cellulose utilizing acid hydrolysis. The rod-like structure of CNC was observed by TEM and the dimensional characteristics were determined by TEM, DLS and AFM. CNC lengths obtained by TEM analysis were significantly lower than values obtained from DLS and AFM. CNCs from commercial cellulose were the longest, compared to acacia (smallest), eucalyptus and pine CNCs.

All samples increased in crystallinity indicating that amorphous areas have been efficiently dissolved from crystalline regions, resulting in CNCs. Acacia showed the highest crystallinity compared to commercial CNCs, which displayed the lowest crystallinity. However, crystallinity of all CNCs were within a range of 70 to 80 % and no CNC source was significantly superior to the other.

Acacia had the largest CNC yield, closely followed by CNCs from commercial cellulose. Eucalyptus and pine, which displayed significantly lower yields. Literature has shown that larger CNC yields are as a result of higher particle charge densities.

DSC confirmed that CNCs from all sources have the capabilities to be utilised in low current electronic devices, as they displayed a melting temperature more than double the operating temperatures of a typical capacitor. Pine CNCs exhibited the highest melt onset temperature whereas CNCs from commercial cellulose were observed to have the lowest. However, all CNCs are once again not significantly different in this regard.

The source of the commercial cellulose was unknown, but literature suggests that it is obtained predominantly from softwood. Thus, pine was used to as a reference point for commercial cellulose. However, in most analysis, other than XRD and DSC, CNCs from pine exhibited inferior characteristics compared to CNCs from commercial cellulose. Furthermore, no clear difference was determined between hardwoods and softwood CNCs and CNCs synthesised from invasive tree species were found to be similar, if not superior, to CNCs from commercial cellulose.

5.2. Recommendations

The Seifert acetyl-acetone method is a fast and effective method to isolating cellulose, however, it can be optimised to improve the charge density of cellulose by optimising delignification. This has the potential to increase CNC yield as the delignification process has a significant influence on the cellulose charge density. The charge density of the cellulose from the different sources should be analysed to determine the exact effect it has on the CNC yield.

The CNC yield and properties of other invasive wood species could be studied, taking into account the growth conditions, to determine the environmental effects.

The processes used to isolate cellulose and CNC by means of Seifert acetyl-acetone and acid hydrolysis, respectively, are expensive and more importantly environmentally unfriendly, as large amounts of toxic chemicals become waste products. For the isolation of cellulose utilising the Seifert method, chemical could potentially be reused if they are distilled after every step- as they have very low evaporation temperatures. Whereas with the synthesis of CNCs, a more cost effective and non-toxic alternative would be to produce CNCs via microfluidization or homogenization.

References

Abas, Z., Kim, H. S., Kim, J., & Kim, J.-H. (2014). Cellulose Electro-Active Paper: From Discovery to Technology Applications. *Frontiers in Materials*, *1*(September), 1–4. https://doi.org/10.3389/fmats.2014.00017

Abdul Khalil, H. P. S., Bhat, A. H., & Ireana Yusra, A. F. (2012). Green composites from sustainable cellulose nanofibrils: A review. *Carbohydrate Polymers*, *87*(2), 963–979. https://doi.org/10.1016/j.carbpol.2011.08.078

Araki, J., Wada, M., Kuga, S., & Okano, T. (1998). Flow properties of microcrystalline cellulose suspension prepared by acid treatment of native cellulose. *Colloids and Surfaces A: Physicochemical and Engineering Aspects*, *142*(1), 75–82. https://doi.org/10.1016/S0927-7757(98)00404-X

Beck-Candanedo, S., Roman, M., & Gray, D. G. (2005). Effect of reaction conditions on the properties and behavior of wood cellulose nanocrystal suspensions. *Biomacromolecules*, *6*(2), 1048–1054. https://doi.org/10.1021/bm049300p

Boisset, C., Chanzy, H., Henrissat, B., Lamed, R., Shoham, Y., & Bayer, E. A. (1999). thermocellum cellulosome : structural and morphological aspects, *340*, 829–835.

Bondeson, D., Mathew, A., & Oksman, K. (2006). Optimization of the isolation of nanocrystals from microcrystalline cellulose by acid hydrolysis. *Cellulose*, *13*(2), 171–180. https://doi.org/10.1007/s10570-006-9061-4

Carrasco, G., Yu, Y., & Diserud, O. (2011). Quantitative electron microscopy of cellulose nanofibril structures from Eucalyptus and Pinus radiata kraft pulp fibers. *Microscopy and Microanalysis : The Official Journal of Microscopy Society of America, Microbeam Analysis Society, Microscopical Society of Canada*, *17*(4), 563–571. https://doi.org/10.1017/S1431927611000444

Chen, W., Yu, H., Liu, Y., Chen, P., Zhang, M., & Hai, Y. (2011). Individualization of cellulose nanofibers from wood using high-intensity ultrasonication combined with chemical pretreatments. *Carbohydrate Polymers*, *83*(4), 1804–1811. https://doi.org/10.1016/j.carbpol.2010.10.040

Chen, W., Yu, H., Liu, Y., Hai, Y., Zhang, M., & Chen, P. (2011). Isolation and characterization of cellulose nanofibers from four plant cellulose fibers using a chemical-ultrasonic process. *Cellulose*, *18*(2), 433–442. https://doi.org/10.1007/s10570-011-9497-z

Cherian, B. M., Leão, A. L., De Souza, S. F., Costa, L. M. M., De Olyveira, G. M., Kottaisamy, M., … Thomas, S. (2011). Cellulose nanocomposites with nanofibres isolated from pineapple leaf fibers for medical applications. *Carbohydrate Polymers*, *86*(4), 1790–1798. https://doi.org/10.1016/j.carbpol.2011.07.009

Cherian, B. M., Leão, A. L., de Souza, S. F., Thomas, S., Pothan, L. A., & Kottaisamy, M. (2010). Isolation of nanocellulose from pineapple leaf fibres by steam explosion. *Carbohydrate Polymers*, *81*(3), 720–725. https://doi.org/10.1016/j.carbpol.2010.03.046

Chinga-Carrasco, G., Tobjörk, D., & Österbacka, R. (2012). Inkjet-printed silver nanoparticles on nano-engineered cellulose films for electrically conducting structures and organic transistors: concept and challenges. *Journal of Nanoparticle Research*, *14*(11), 1213. https://doi.org/10.1007/s11051-012-1213-x

Clemons, C. M. (2010). Natural Fibers. In M. Xanthos (Ed.), *Functional Fillers for Plastics* (2nd ed., pp. 213–223). Wiley-VCH Verlag GmbH.

Clorius, C. O. (2002). *Fatigue in Wood*. Denmark.

Couderc, S., Ducloux, O., Kim, B. J., & Someya, T. (2009). A mechanical switch device made of a polyimide-coated microfibrillated cellulose sheet. *Journal of Micromechanics and Microengineering*, *19*(5), 55006. https://doi.org/10.1088/0960-1317/19/5/055006

Cown, D. J., & McConchie, D. (1981). Effects of thinning and fertiliser application on wood properties of Pinus radiata. *New Zealand Journal of Forestry Science*, (April), 79–91.

Craig, M., Caulfield, C., & Caulfield, D. (2005). Functional Fillers for Plastics. In M. Xanthos (Ed.), *Functional Fillers for Plastics* (pp. 250–270). Federal Republic of Germany: Strauss GmbH, Mörlenbach.

Credou, J., & Berthelot, T. (2015). Cellulose: from biocompatible to bioactive material. *Materials Chemistry B*, *2*, 4767–4788. https://doi.org/10.1039/c4tb00431k

Cristian Neagu, R., Kristofer Gamstedt, E., Bardage, S. L., & Lindström, M. (2006). Ultrastructural features affecting mechanical properties of wood fibres. *Wood Material Science and Engineering*, *1*(3–4), 146–170. https://doi.org/10.1080/17480270701195374

Csoka, L., Hoeger, I. C., Rojas, O. J., Peszlen, I., Pawlak, J. J., & Peralta, P. N. (2012). Piezoelectric Effect of Cellulose Nanocrystals Thin Films. *ACS Macro Letters*, *1*(7), 867–870. https://doi.org/10.1021/mz300234a

DAFF. (2015). *Strategic Plan*. (F. and F. Department of Agriculture, Ed.). Department of

Agriculture, Forestry and Fisheries.

DEA. (2014). No Title. *A National Strategy for Dealing with Biological Invasion in South Africa*.

De Mesquita, J. P., Donnici, C. L., & Pereira, F. V. (2010). Biobased nanocomposites from layer-by-layer assembly of cellulose nanowhiskers with chitosan. *Biomacromolecules*, *11*(2), 473–480. https://doi.org/10.1021/bm9011985

Dong, X. M., Revol, J., & Gray, D. G. (1998). No Title. *Cellulose*, *5*(1), 19–32. https://doi.org/10.1023/A:1009260511939

du Toit, M. L. (2013). *Incorporation of polysaccharide nanowhiskers into a poly (ethylene-co-vinyl alcohol) matrix*. University of Stellenbosch.

Dubilier, C. (2011). Aluminum Electrolytic Capacitor Application Guide. *Technology*, (864), 1–22. Retrieved from http://www.cde.com/resources/catalogs/AEappGUIDE.pdf

Durán, N., Lemes, A. P., Durán, M., Freer, J., & Baeza, J. (2011). A minireview of cellulose nanocrystals and its potential integration as co-product in bioethanol production. *Journal of the Chilean Chemical Society*, *56*(2), 672–677. https://doi.org/10.4067/S0717-97072011000200011

Fall, A. B., Burman, A., & Wågberg, L. (2014). Cellulosic nanofibrils from eucalyptus, acacia and pine fibers. *Special Issue: NANOCELLULOSE Nordic Pulp & Paper Research Journal*, *29*(1).

Fang, Z., Zhu, H., Yuan, Y., Ha, D., Zhu, S., Preston, C., … Hu, L. (2014). Novel Nanostructured Paper with Ultrahigh Transparency and Ultrahigh Haze for Solar Cells. *Nano Letters*, *14*(2), 765–773. https://doi.org/10.1021/nl404101p

Gaspar, D., Fernandes, S. N., de Oliveira, A. G., Fernandes, J. G., Grey, P., Pontes, R. V, … Fortunato, E. (2014). Nanocrystalline cellulose applied simultaneously as the gate dielectric and the substrate in flexible field effect transistors. *Nanotechnology*, *25*(9), 94008. https://doi.org/10.1088/0957-4484/25/9/094008

George, J., & Sabapathi, S. (2015). Cellulose nanocrystals: synthesis , functional properties , and applications. *Nanotechnology, Science and Applications*, *8*, 45–54.

Grange, M. (2015). The use of fluorescence to probe the morphology changes in complex polymers Marehette le Grange, (March).

Habibi, Y., Lucia, L. A., & Rojas, O. J. (2010). Cellulose nanocrystals: Chemistry, self-assembly, and applications. *Chemical Reviews*, *110*(6), 3479–3500. https://doi.org/10.1021/cr900339w

Heath, L., & Thielemans, W. (2010). Cellulose nanowhisker aerogels. *Green Chemistry*, *12*(8), 1448. https://doi.org/10.1039/c0gc00035c

Henderson, L. (2007). Invasive, naturalized and casual alien plants in southern Africa: A summary based on the Southern African Plant Invaders Atlas (SAPIA). *Bothalia*, *37*(2), 215–248. https://doi.org/10.4102/abc.v37i2.322

Hoo, C. M., Starostin, N., West, P., & Mecartney, M. L. (2008). A comparison of atomic force microscopy (AFM) and dynamic light scattering (DLS) methods to characterize nanoparticle size distributions. *Journal of Nanoparticle Research*, *10*(S1), 89–96. https://doi.org/10.1007/s11051-008-9435-7

Hsu, L., Weder, C., & Rowan, S. J. (2011). Stimuli-responsive, mechanically-adaptive polymer nanocomposites. *J. Mater. Chem.*, *21*(9), 2812–2822. https://doi.org/10.1039/C0JM02383C

Hu, L., Liu, N., Eskilsson, M., Zheng, G., McDonough, J., Wågberg, L., & Cui, Y. (2013). Silicon-conductive nanopaper for Li-ion batteries. *Nano Energy*, *2*(1), 138–145. https://doi.org/10.1016/j.nanoen.2012.08.008

Hubbell, C. A., & Ragauskas, A. J. (2010). Bioresource Technology Effect of acid-chlorite delignification on cellulose degree of polymerization. *Bioresource Technology*, *101*(19), 7410–7415. https://doi.org/10.1016/j.biortech.2010.04.029

ISO/TC229. (2017). *Nanotechnologies — Standard terms and their definition for cellulose nanomaterial*. *ISO/TS 20477:2017(E)*. Retrieved from https://www.evs.ee/preview/iso-ts-20477-2017-en.pdf

Jeon, J.-H., Oh, I.-K., Kee, C.-D., & Kim, S.-J. (2010). Bacterial cellulose actuator with electrically driven bending deformation in hydrated condition. *Sensors and Actuators B: Chemical*, *146*(1), 307–313. https://doi.org/10.1016/j.snb.2010.02.046

John, M. J., & Thomas, S. (2008). Biofibres and biocomposites. *Carbohydrate Polymers*, *71*(3), 343–364. https://doi.org/10.1016/j.carbpol.2007.05.040

Kargarzadeh, H., Ahmad, I., Abdullah, I., Dufresne, A., Zainudin, S. Y., & Sheltami, R. M. (2012). Effects of hydrolysis conditions on the morphology, crystallinity, and thermal stability of cellulose nanocrystals extracted from kenaf bast fibers. *Cellulose*, *19*(3), 855–866. https://doi.org/10.1007/s10570-012-9684-6

Kaushik, M., Fraschini, C., Chauve, G., Putaux, J.-L., & Moores, A. (2015a). Transmission Electron Microscopy for the Characterization of Cellulose Nanocrystals. In *The Transmission Electron*

Microscope - Theory and Applications. InTech. https://doi.org/10.5772/60985

Kaushik, M., Fraschini, C., Chauve, G., Putaux, J.-L., & Moores, A. (2015b). Transmission Electron Microscopy for the Characterization of Cellulose Nanocrystals. In *The Transmission Electron Microscope - Theory and Applications*. InTech. https://doi.org/10.5772/60985

Kaushik, M., & Moores, A. (2016). Review: nanocelluloses as versatile supports for metal nanoparticles and their applications in catalysis. *Green Chem.*, *18*(3), 622–637. https://doi.org/10.1039/C5GC02500A

Khan, A., Vu, K. D., Chauve, G., Bouchard, J., Riedl, B., & Lacroix, M. (2014). Optimization of microfluidization for the homogeneous distribution of cellulose nanocrystals (CNCs) in biopolymeric matrix. *Cellulose*, 3457–3468. https://doi.org/10.1007/s10570-014-0361-9

Khatkar. (2015). Hardwoods and Softwoods starter/plenary. Retrieved November 4, 2017, from https://www.tes.com/teaching-resource/hardwoods-and-softwoods-starter-plenary-7525723

Klemm, D., Heublein, B., Fink, H. P., & Bohn, A. (2005). Cellulose: Fascinating biopolymer and sustainable raw material. *Angewandte Chemie - International Edition*, *44*(22), 3358–3393. https://doi.org/10.1002/anie.200460587

Kollmann, F. (1968). chemical composition of wood. *Principles of Wood Science and Technology* ©.

Kretschmann, D. (2003). David kretschmann, 775–776.

Kudo, K., Nabeshima, E., Begum, S., Yamagishi, Y., Nakaba, S., Oribe, Y., … Funada, R. (2014). The effects of localized heating and disbudding on cambial reactivation and formation of earlywood vessels in seedlings of the deciduous ring-porous hardwood, Quercus serrata. *Annals of Botany*, *113*(6), 1021–1027. https://doi.org/10.1093/aob/mcu026

Kumar, R., Singh, S., & Singh, O. V. (2008). Bioconversion of lignocellulosic biomass : biochemical and molecular perspectives, *35*, 377–391. https://doi.org/10.1007/s10295-008-0327-8

Lahiji, R. R., Xu, X., Reifenberger, R., Raman, A., Rudie, A., & Moon, R. J. (2010). Atomic Force Microscopy Characterization of Cellulose Nanocrystals. *Langmuir*, *26*(6), 4480–4488. https://doi.org/10.1021/la903111j

Le Maitre, D. B., Versefeld, D., & Chapman, R. (2000). The impact of invading alien plants on surface water resources in South Africa : A preliminary assessment. *Water SA Vol.*, *26*(3), 397–408. Retrieved from http://www.wrc.org.za

Leijonmarck, S., Cornell, A., Lindbergh, G., & Wågberg, L. (2013). Single-paper flexible Li-ion battery cells through a paper-making process based on nano-fibrillated cellulose. *Journal of Materials Chemistry A*, *1*(15), 4671. https://doi.org/10.1039/c3ta01532g

Liew, S. Y., Thielemans, W., & Walsh, D. A. (2010). Electrochemical Capacitance of Nanocomposite Polypyrrole / Cellulose Films. *Journal of Materials Chemistry C*, *114*, 17926–17933.

Lu, S., Li, L., & Zhou, G. (2017). Genetic modification of wood quality for second- generation biofuel production, *1*(4), 230–236. https://doi.org/10.4161/gmcr.1.4.13486

Lundqvist, S., Grahn, T., Olsson, L., & Seifert, T. (2017). Comparison of wood , fibre and vessel properties of drought-tolerant eucalypts in South Africa. *Southern Forests: A Journal of Forest Science*, *79*(November), 215–225. https://doi.org/10.2989/20702620.2016.1254910

Lynd, L., Weimer, P., van Zyl, W., & Pretorius, I. (2002). Pesquisa Nacional de Saneamento Básico 2008. *Bioresource Technology*, *66*(3), 506–577. https://doi.org/10.1128/MMBR.66.3.506

MacFarlane, C., Warren, C. R., White, D. A., & Adams, M. A. (1999). A rapid and simple method for processing wood to crude cellulose for analysis of stable carbon isotopes in tree rings. *Tree Physiology*, *19*(12), 831–835. https://doi.org/10.1093/treephys/19.12.831

Maiti, R., & Rodriguez, H. (2015). Forest Research Wood Anatomy Could Predict the Adaptation of Woody Plants to Environmental Stresses and Quality of Timbers. *Open Access Journal Volume*, *4*(4). https://doi.org/10.4172/2168-9776.1000e121

Mandal, A., & Chakrabarty, D. (2011). Isolation of nanocellulose from waste sugarcane bagasse (SCB) and its characterization. *Carbohydrate Polymers*, *86*(3), 1291–1299. https://doi.org/10.1016/j.carbpol.2011.06.030

Marais, C., Turpie, J., Mullins, D., Conradie, B., Khan, A., Goldin, J., … Ndzinge, V. (2001). A cost-benefit analysis framework for the national Working for Water Programme. *… to Working for Water*, (December).

Martinez, A., Speranza, M., Ruiz-dueñas, F. J., Ferreira, P., Camarero, S., Guillén, F., … Río, J. C. (2005). Biodegradation of lignocellu- losics : microbial , chemical , and enzymatic aspects of the fungal attack of lignin, 195–204.

Mazzarello, P. (1999). A unifying concept: the history of cell theory. *Nature Cell Biology*, *1*(1), E13--5. https://doi.org/10.1038/8964

Mckendry, P. (2002). Energy production from biomass (part 1): overview of biomass. *Bioresource Technology*, *83*(July 2001), 37–46.

Meyer, G., & Amer, N. M. (1988a). Erratum: Novel optical approach to atomic force microscopy. *Applied Physics Letters*, *53*(24), 2400–2402. https://doi.org/10.1063/1.100425

Meyer, G., & Amer, N. M. (1988b). Erratum: Novel optical approach to atomic force microscopy. *Applied Physics Letters*, *53*(24), 2400–2402. https://doi.org/10.1063/1.100425

Miller, R. B. (1999). *Structure of Wood*. *Wood handbook—Wood as an engineering material*. Madison, WI. Retrieved from http://www.civil.uwaterloo.ca/beg/ce265/woodhandbook_extracts.pdf

Morais, J. P. S., Rosa, M. D. F., De Souza Filho, M. D. S. M., Nascimento, L. D., Do Nascimento, D. M., & Cassales, A. R. (2013). Extraction and characterization of nanocellulose structures from raw cotton linter. *Carbohydrate Polymers*, *91*(1), 229–235. https://doi.org/10.1016/j.carbpol.2012.08.010

Morán, J., Alvarez, V. A., Cyras, V. P., & Vazquez, A. (2008). Extraction of cellulose and preparation of nanocellulose from sisal fibers. *Cellulose*, *15*(August 2014), 149–159. https://doi.org/10.1007/s10570-007-9145-9

Morán, J., Alvarez, V., Cyras, V., & Vázquez, A. (2008). Extraction of cellulose and preparation of nanocellulose from sisal fibers. *Cellulose*, *15*(1), 149–159. https://doi.org/10.1007/s10570-007-9145-9

Morelli, C. L., Marconcini, J. M., Pereira, F. V., Bretas, R. E. S., & Branciforti, M. C. (2012). Extraction and characterization of cellulose nanowhiskers from balsa wood. *Macromolecular Symposia*, *319*(1), 191–195. https://doi.org/10.1002/masy.201100158

Museochies.it. (2017). Wood reference plane. Retrieved October 29, 2017, from http://museochies.it/1ingl_museo/38legnoE.html

Nel, J. L., Richardson, D. M., Rouget, M., Mgidi, T. N., Mdzeke, N., Maitre, D. C. Le, … Neser, S. (2004). A proposed classification of invasive alien plant species in South Africa : towards prioritizing species and areas for management action, (February), 53–64.

Nunlist, T. (2012). Understanding Wood: Four Structure Types. Retrieved November 9, 2017, from https://www.popularwoodworking.com/techniques/understanding-wood-four-structure-types

Orts, W. J., Shey, J., Imam, S. H., Glenn, G. M., Guttman, M. E., & Revol, J. F. (2005). Application of cellulose microfibrils in polymer nanocomposites. *Journal of Polymers and the*

Environment, *13*(4), 301–306. https://doi.org/10.1007/s10924-005-5514-3

Österberg, M., & Cranston, E. D. (2016). Special issue on nanocellulose Special issue on nanocellulose- Editorial. *Nordic Pulp & Paper Research Journal*, *29*(January 2014), 1–3.

Oyeniyi, Y. J., & Itiola, O. A. (2012). The physicochemical characteristic of microcrystalline cellulose, derived from sawdust, agricultural waste products. *International Journal of Pharmacy and Pharmaceutical Sciences*, *4*(SUPPL.1), 197–200.

Patrício, P. S. D. O., Pereira, F. V., Dos Santos, M. C., De Souza, P. P., Roa, J. P. B., & Orefice, R. L. (2013). Increasing the elongation at break of polyhydroxybutyrate biopolymer: Effect of cellulose nanowhiskers on mechanical and thermal properties. *Journal of Applied Polymer Science*, *127*(5), 3613–3621. https://doi.org/10.1002/app.37811

Pearson, R. G., & Dawson, T. P. (2005). Long-distance plant dispersal and habitat fragmentation: Identifying conservation targets for spatial landscape planning under climate change. *Biological Conservation*, *123*(3), 389–401. https://doi.org/10.1016/j.biocon.2004.12.006

Pecora, R. (2000). Dynamic light scattering measurement of nanometer particles in liquids. *Journal of Nanoparticle Research*, *2*(2), 123–131. https://doi.org/10.1023/A:1010067107182

Pérez, J., Muñoz-Dorado, J., De La Rubia, T., & Martínez, J. (2002). Biodegradation and biological treatments of cellulose, hemicellulose and lignin: An overview. *International Microbiology*, *5*(2), 53–63. https://doi.org/10.1007/s10123-002-0062-3

Petersson, L., Kvien, I., & Oksman, K. (2007). Structure and thermal properties of poly(lactic acid)/cellulose whiskers nanocomposite materials. *Composites Science and Technology*, *67*(11–12), 2535–2544. https://doi.org/10.1016/j.compscitech.2006.12.012

Pettersen, R. (1984). *The Chemistry of Solid Wood*. (R. Rowell, Ed.), *The chemistry of solid wood* (Vol. 207). Washington, DC: American Chemical Society. https://doi.org/10.1021/ba-1984-0207

Pettersen, R. C. (1984). The Chemical Composition of Wood. *THE CHEMISTRY OF SOLID WOOD*, 58–125.

Pitelka, L. (1997). Plant Migration and Climate Change. *American Scientist*, *85*, 464–473. Retrieved from http://www.jstor.org.proxy.library.ohio.edu/stable/pdf/27856854.pdf?refreqid=excelsior:d35b9467140e5db1e0a05a64de352dda

Pittermann, J., Sperry, J. S., Wheeler, J. K., Hacke, U. G., & Sikkema, E. H. (2006). Mechanical

reinforcement of tracheids compromises the hydraulic efficiency of conifer xylem. *Plant, Cell and Environment*, *50*(29), 1618–1628. https://doi.org/10.1111/j.1365-3040.2006.01539.x

Plants, W. O. F., M, M., Darv, A. G., Fry, S. C., & Peter, A. (1984). STRUCTURE AND FUNCTION OF THE PRIMARY CELL WALLS OF PLANTS, *53*, 625–630.

Plomion, C., Leprovost, G., & Stokes, A. (2001). Wood Formation in Trees Wood Formation in Trees. *Plant Physiology*, *127*(December), 1513–1523. https://doi.org/10.1104/pp.010816.1

Pooley, S. (2009). Jan van riebeeck as pioneering explorer and conservator of natural resources at the cape of good hope (1652-62). *Environment and History*, *15*(1), 3–33. https://doi.org/10.3197/096734009X404644

Pu, Y., Zhang, D., Singh, P. M., & Ragauskas, A. J. (2008). The new forestry biofuels sector, *2*, 58–73. https://doi.org/10.1002/bbb

Pu, Y., Zhang, J., Elder, T., Deng, Y., Gatenholm, P., & Ragauskas, A. J. (2007). Investigation into nanocellulosics versus acacia reinforced acrylic films. *Composites Part B: Engineering*, *38*(3), 360–366. https://doi.org/10.1016/j.compositesb.2006.07.008

Reventós, M., Rius, J., & Amigó, J. (1912). MINERALOGY AND GEOLOGY : THE ROLE OF CRYSTALLOGRAPHY SINCE THE DISCOVERY OF X-RAY DIFFRACTION IN 1912, *25*(2012), 133–143.

Richardson, D. M., & Wilgen, B. W. Van. (2004). Invasive alien plants in South Africa : how well do we understand the ecological impacts ? *South African Journal of Science*, *100*(February), 45–52.

Rusli, R., Shanmuganathan, K., Rowan, S. J., Weder, C., & Eichhorn, S. J. (2010). Stress-Transfer in Anisotropic and Environmentally Adaptive Cellulose Whisker Nanocomposites. *Biomacromolecules*, *11*(3), 762–768.

Rusli, R., Shanmuganathan, K., Rowan, S. J., Weder, C., & Eichhorn, S. J. (2011). Stress Transfer in Cellulose Nanowhisker Composites—Influence of Whisker Aspect Ratio and Surface Charge. *Biomacromolecules*, *12*(4), 1363–1369. https://doi.org/10.1021/bm200141x

Sabinesh, S., Renald, C., & Sathish, S. (2014). Investigation on Tensile and Flexural properties of Cotton Fiber Reinforced Isophthallic Polyester Composites, (2), 213–219. Retrieved from http://inpressco.com/category/ijcet

Sabo, R., Yermakov, A., Law, C. T., & Elhajjar, R. (2016). Nanocellulose-Enabled Electronics, Energy Harvesting Devices, Smart Materials and Sensors: A Review. *Journal of Renewable*

Materials, *4*(5), 297–312. https://doi.org/10.7569/JRM.2016.634114

Sacui, I. A., Nieuwendaal, R. C., Burnett, D. J., Stranick, S. J., Jorfi, M., Weder, C., … Gilman, J. W. (2014). Comparison of the Properties of Cellulose Nanocrystals and Cellulose Nanofibrils Isolated from Bacteria, Tunicate, and Wood Processed Using Acid, Enzymatic, Mechanical, and Oxidative Methods. *ACS Applied Materials & Interfaces*, *6*(9), 6127–6138. https://doi.org/10.1021/am500359f

Samuel, V., & Samuel, L. (2010). Moisture Relations and Physical Properties of CHAPTER 4 Moisture Relations and Physical Properties of Wood, (March 2015).

Sap, K. A., Demmers, J. A. A., Bocchiaro, P., Zamperini, A., Sap, K. A., & Demmers, J. A. A. (2011). *Atherosclerotic Cardiovascular Disease*. (K. Pesek, Ed.), *Intech* (Vol. 6). InTech. https://doi.org/10.5772/711

Savadekar, N. R., & Mhaske, S. T. (2012). Synthesis of nano cellulose fibers and effect on thermoplastics starch based films. *Carbohydrate Polymers*, *89*(1), 146–151. https://doi.org/10.1016/j.carbpol.2012.02.063

Segal, L., Creely, J., Martin, A., & Conrad, C. (1959). An Empirical Method for Estimating the Degree of Crystallinity of Native Cellulose Using the X-Ray Diffractometer. *Textile Research Journal*, *29*(10), 786–794. https://doi.org/10.1177/004051755902901003

Seo, J., Chang, T., Lee, J., Sabo, R., Zhou, W., Cai, Z., & Gong, S. (2015). Microwave flexible transistors on cellulose nanofibrillated fiber substrates Microwave flexible transistors on cellulose nanofibrillated fiber substrates, *262101*(2015), 0–4. https://doi.org/10.1063/1.4921077

Shaughnessy, G. (1980). Historical ecology of alien woody plants in the vicinity of Cape Town, South Africa. https://doi.org/citeulike-article-id:13504672

Shmulsky, R., & Jones, P. (2011). hardwood structures. In *Forest Products and Wood Science* (6th ed., pp. 79–106). Oxford: Wiley-Blackwell. https://doi.org/10.1002/9780470960035.ch5

Showers, K. B. (2010). Prehistory of Southern African Forestry: From vegetable garden to tree plantation. *Environment and History*, *16*(3), 295–322. https://doi.org/10.3197/096734010X519771

Siqueira, G., Bras, J., & Dufresne, A. (2010). Cellulosic Bionanocomposites: A Review of Preparation, Properties and Applications, *2*(i), 728–765. https://doi.org/10.3390/polym2040728

Sofla, M. R. K., Brown, R. J., Tsuzuki, T., & Rainey, T. J. (2016). A comparison of cellulose nanocrystals and cellulose nanofibres extracted from bagasse using acid and ball milling methods. *Advances in Natural Sciences: Nanoscience and Nanotechnology*, *7*(3), 35004. https://doi.org/10.1088/2043-6262/7/3/035004

Tampone, G. (2007). Mechanical Failures of the Timber Structural Systems, (November).

Teters, C., Kong, W., Taylor, M., Simonsen, J., Lerner, M., Plant, T., & Evans, G. (2007). The cellulose nanocrys- tal electro-optic effect, in: International Conference on Nanotechnology for the Forest Products Industry (p. 49). Knoxville. Retrieved from papers3://publication/uuid/965654D7-15A2-49EA-AAC1-B8239E72185B

Thornber, J. P., & Notrhcote, D. H. (1961). Changes in the Chemical Composition of a Cambial Cell during its Differentiation into Xylem and Phloem Tissue in Trees. *Biochemical Journal*, *81*(Table 3), 449–455.

Tsoumis, G. (1991). *Science and Technology of Wood Structure, Properties, Utilization*.

Uggla, C., Magel, E., Moritz, T., & Sundberg, B. (2001). Function and Dynamics of Auxin and Carbohydrates during Earlywood / Latewood Transition in Scots Pine 1. *Plant Physiol*, *125*, 2029–2039.

van Wilgen, B., De Wit, M. P., Anderson, H. J., le Maitre, D. C., Kotze, I. M., Ndala, S., … Rapholo, M. B. (2004). Costs and benefits of biological control of invasive alien plants: Case studies from South Africa. *South African Journal of Science*. Retrieved from http://reference.sabinet.co.za/sa_epublication_article/sajsci_v100_n1_2_a24

van Wilgen, B. W., Forsyth, G. G., Le Maitre, D. C., Wannenburgh, A., Kotzé, J. D. F., van den Berg, E., & Henderson, L. (2012). An assessment of the effectiveness of a large, national-scale invasive alien plant control strategy in South Africa. *Biological Conservation*, *148*(1), 28–38. https://doi.org/10.1016/j.biocon.2011.12.035

Van Wilgen, B. W., Richardson, D. M., le Maitre, D. C., Marais, C., Magadlela, D., Wilgen, B. W. V. a N., & Maitre, D. C. L. E. (2001). The economic consequences of alien plant invasions: examples of impacts and approaches to sustainable management in South Africa. *Environment, Development and Sustainability*, *3*, 145–168. https://doi.org/10.1023/A:1011668417953

Villanova, J. C. O., Ayres, E., Carvalho, S. M., Patrício, P. S., Pereira, F. V., & Oréfice, R. L. (2011). Pharmaceutical acrylic beads obtained by suspension polymerization containing cellulose nanowhiskers as excipient for drug delivery. *European Journal of Pharmaceutical*

Sciences, *42*(4), 406–415. https://doi.org/10.1016/j.ejps.2011.01.005

Wang, B., Sain, M., & Oksman, K. (2007). Study of structural morphology of hemp fiber from the micro to the nanoscale. *Applied Composite Materials*, *14*(2), 89–103. https://doi.org/10.1007/s10443-006-9032-9

Wang, Z. L. (2000a). Transmission Electron Microscopy of Shape-Controlled Nanocrystals and Their Assemblies. *The Journal of Physical Chemistry B*, *104*(6), 1153–1175. https://doi.org/10.1021/jp993593c

Wang, Z. L. (2000b). Transmission Electron Microscopy of Shape-Controlled Nanocrystals and Their Assemblies. *The Journal of Physical Chemistry B*, *104*(6), 1153–1175. https://doi.org/10.1021/jp993593c

Yagyu, H., Saito, T., Isogai, A., Koga, H., & Nogi, M. (2015). Chemical Modification of Cellulose Nanofibers for the Production of Highly Thermal Resistant and Optically Transparent Nanopaper for Paper Devices. *ACS Applied Materials & Interfaces*, *7*(39), 22012–22017. https://doi.org/10.1021/acsami.5b06915

Yang, X., Shi, K., Zhitomirsky, I., & Cranston, E. D. (2015). Cellulose Nanocrystal Aerogels as Universal 3D Lightweight Substrates for Supercapacitor Materials. *Advanced Materials*, *27*(40), 6104–6109. https://doi.org/10.1002/adma.201502284

Ylmén, R., Jäglid, U., Steenari, B.-M., & Panas, I. (2009). Early hydration and setting of Portland cement monitored by IR, SEM and Vicat techniques. *Cement and Concrete Research*, *39*(5), 433–439. https://doi.org/10.1016/j.cemconres.2009.01.017

Yu, H., Qin, Z., Liang, B., Liu, N., Zhou, Z., & Chen, L. (2013). Facile extraction of thermally stable cellulose nanocrystals with a high yield of 93% through hydrochloric acid hydrolysis under hydrothermal conditions. *Journal of Materials Chemistry A: Materials for Energy and Sustainability*, *1*(Copyright (C) 2015 American Chemical Society (ACS). All Rights Reserved.), 3938–3944. https://doi.org/10.1039/c3ta01150j

Yuldoshov, S., Atakhanov, A., & Rashidova, S. (2016). Cotton Cellulose, Microcrystalline Cellulose and Nanocellulose: Carboxymethylation and Oxidation Reaction Activity. *Nano Sci Nano Technol*, *10*(6), 106. Retrieved from http://www.tsijournals.com/articles/cotton-cellulose-microcrystalline-cellulose-and-nanocellulose-carboxymethylation-and-oxidation-reaction-activity.html

ZAKARIA, M., SHAHRODIN, M., GHAFAR, M., BAHRI, S., & YUSOF, K. (2013). Timber Introduction in Building.

Zhang, C., Dan, Y., Peng, J., Turng, L.-S., Sabo, R., & Clemons, C. (2014). Thermal and Mechanical Properties of Natural Rubber Composites Reinforced with Cellulose Nanocrystals from Southern Pine. *Advances in Polymer Technology*, *33*(S1), n/a-n/a. https://doi.org/10.1002/adv.21448

Zhang, W., He, X., Li, C., Zhang, X., Lu, C., Zhang, X., & Deng, Y. (2014). High performance poly (vinyl alcohol)/cellulose nanocrystals nanocomposites manufactured by injection molding. *Cellulose*, *21*(1), 485–494. https://doi.org/10.1007/s10570-013-0141-y

Zhou, C., Shi, Q., Guo, W., Terrell, L., Qureshi, A. T., Hayes, D. J., & Wu, Q. (2013). Electrospun Bio-Nanocomposite Scaffolds for Bone Tissue Engineering by Cellulose Nanocrystals Reinforcing Maleic Anhydride Grafted PLA. *ACS Applied Materials & Interfaces*, *5*(9), 3847–3854. https://doi.org/10.1021/am4005072

Zhou, C., Wu, Q., Yue, Y., & Zhang, Q. (2011). Application of rod-shaped cellulose nanocrystals in polyacrylamide hydrogels. *Journal of Colloid and Interface Science*, *353*(1), 116–123. https://doi.org/10.1016/j.jcis.2010.09.035

Zhou, Y., Fuentes-Hernandez, C., Khan, T. M., Liu, J.-C., Hsu, J., Shim, J. W., … Kippelen, B. (2013). Recyclable organic solar cells on cellulose nanocrystal substrates. *Scientific Reports*, *3*(1), 1536. https://doi.org/10.1038/srep01536